

Mount Suhora high cadence photometric survey of T Tauri-type starsMichał Siwak, Marek Drózdź, Karol Gut, Maciej Winiarski, Waldemar
Ogłóza, Grzegorz StachowskiMount Suhora Astronomical Observatory, Cracow Pedagogical University,
ul. Podchorążych 2, 30-084 Kraków
e-mail: michal.siwak@gmail.com*Received Month Day, Year*

ABSTRACT

Results of high-cadence multi-colour observations of 121 pre-main sequence stars available from the northern hemisphere are presented. The aim of this survey was to detect transit-like signatures caused by occultation of these young stars and their accretion-induced hot spots by close-in planets and/or dusty clumps. Although none planetary transits were detected, our data allow to determine rotational periods for some T Tauri stars, characterise accretion processes operating in classical T Tauri-type stars in time scales ranging from a few minutes to days, as well as the large-scale dips caused by dusty warped discs.

Key words: *T Tauri stars, Herbig Ae/Be stars, accretion*

1. Introduction

Followed by Class 0 and Class I protostar phases lasting about 10^5 yr, classical T Tauri-type stars (CTTS) and their more massive ($\sim 2 - 10 M_{\odot}$) counterparts - Herbig Ae/Be (HAEBE) stars - represent the first observable in visual wavelengths phases of young stars, still being surrounded by accretion discs. Currently it is well observationally established that accretion onto the central star occurs through magnetically controlled accretion, in a way originally proposed for neutron stars by Ghost & Lamb (1977) and further suggested to apply to CTTS by Königl (1991). According to this mechanism, accretion disc is threaded by stellar magnetic field lines. The star-disc locking through magnetic field prevents the star to accelerate its rotation while it contracts well before reaching the breakup speed; instead its rotational period is equalized to the Keplerian period at the disc co-rotation radius. In the narrow transition zone, extending for a few stellar radii from an inner disc radius, the disc plasma is controlled in its motion by the magnetic field and transferred along its lines to the high and moderate stellar latitudes, where it strikes the photosphere producing hot spots. It is normally assumed that the hot spots, together

with solar-type, but huge dark spots produce complex, large amplitude (1-2 mag) photometric variability of the stars (Herbst et al., 1994, 2002). The hot accretion spots are responsible for many peculiarities observed in CTTS, particularly the ultraviolet and visual excess of radiation (veiling) and strong and variable emission lines. While accretion is the dominant mechanism responsible for variability of stars observed well above the disc plane, in stars observed closer to its plane persistent dusty disc warps often cause semi-periodic or variable obscuration of central stars, in combination with the aforementioned accretion-induced variability (e.g. Bouvier et al., 2003; Stauffer et al., 2015; McGinnis et al., 2015; Ansdell et al., 2016).

Hot and cold spots on CTTS should last sufficiently long on stellar photosphere to produce periodic light curves dominated by stellar rotation. Instead, the light curves frequently show quasi-periodic variations or no periodicity at all (Herbst et al., 1994, 2002; Grankin et al., 2007; Rucinski et al., 2008; Alencar et al., 2010; Siwak et al., 2011a; Stauffer et al., 2014). The subject of plasma flows in magnetized stars was numerically investigated with three dimensional magneto hydro dynamical (3D MHD) simulations by Romanowa et al. (2004, 2008), Kulkarni & Romanowa (2008, 2009) and Kurosawa & Romanowa (2013). According to the authors of these publications, for magnetospheres a few times the stellar radius in size (but no less than two stellar radii), the accretion from the surrounding disk can occur in either *stable*, *moderately stable* or *unstable regime*. The regime of accretion which is prevalent at a given time is primarily controlled by the mass accretion rate and it may alternate between moderately stable and unstable depending on the actual value of the mass accretion rate (Romanowa & Kulkarni, 2008). Our *MOST* satellite observations have qualitatively confirmed these theoretical findings: for low mass accretion rates, plasma is transported toward the star in two stable funnel flows originating near the disc co-rotation radius, and it strikes the star near its magnetic poles. Two antipodal fairly stable hot spots formed during this process produce fairly regular light curves, revealing rotational period of a star (e.g. in IM Lup, see in Siwak et al., 2016). Once the mass accretion rate becomes higher, the inner disc radius decreases. Instabilities developing in the "inner disc – magnetosphere" boundary produce a few chaotic equatorial tongues, which penetrate through the magnetosphere and produce short-term chaotic hot spots leading to irregular brightness changes, as observed in RU Lup (Siwak et al., 2016) and TW Hya (Rucinski et al., 2008; Siwak et al., 2011a, 2014, 2018). Except of the above, it was recently observationally established that in CTTS accreting in stable regime either "disc-planet" or "disc-low mass companion" interactions may lead to temporary inner disc instabilities and related episodes of inhomogenous accretion, as seen in CI Tau (Biddle et al., 2018), DQ Tau (Tofflemire et al., 2017a, Muzerolle et al., 2019), and TWA 3A (Tofflemire et al., 2017b).

Planet formation processes appear to start when protostars are still deeply hidden behind dust (e.g. Draskowska & Dullemond, 2018) and continues in proto-

planetary discs during the CTTS and HAEBE phase. It is widely accepted that planets form beyond the "snow line", where is cold enough for volatile compounds to condense into solid ice grains either through core accretion (Pollack et al. 1996), or through instabilities in the disc (Boss, 2001). The disc instability mechanism is very efficient in forming giant planets and brown dwarfs due to gravitational fragmentation in outer parts of massive protoplanetary discs after several thousand – 1 Myr. The core accretion is efficient in forming giant gas planets in less massive protoplanetary discs, with typical time scales of about 3-5 Myr. The most recent discoveries of large populations of pebbles in protoplanetary discs initiated works on planet formation via pebble accretion (e.g. Johansen & Lambrechts, 2017). The state-of-art instruments utilizing mid-, far-infrared, sub-mm and mm wavelengths provide numerous observational evidences for ongoing planets formation at distances of 10-100 AU from central stars (e.g. Flaherty et al., 2011; Benisty et al., 2015, Perez et al., 2016, Stolker et al., 2016). As the "snow line" is located on a few astronomical units for Solar-type stars, the new born planets have to interact with the disc material and gradually migrate to new orbits (Nelson & Papaloizou 2003) to explain the orbits of Earth-like planets in Solar System, and tight 0.03-0.1 AU orbits with 3-10 days orbital periods of "Hot Jupiters", commonly discovered around main-sequence stars during the 90s. Orbital parameters of these giant planets were theoretically explained by Romanova & Lovelace (2006), who obtained that for typical misalignment angle between magnetic and rotational axes of the star, the magnetospheric gap could stop inward migration of all planets at 0.05 AU. Discovery of the first Neptun-like planet K2-33b transiting weak-lined T Tauri star (WTTS) with a period of 5.4 days by *Kepler-K2* mission (David et al. 2016) fits well in the above image. After a decade of unsuccessful application of the radial velocity technique (e.g. Crockett et al., 2012; Lagrange et al., 2013) only recently sophisticated methods of removal of features induced by cold spots and plagues in stellar line profiles, allowed to detect possible long-term periodic radial velocity variations in V830 Tau and TAP 26, which are WTTS (Donati et al., 2015, 2016; Yu et al., 2017), and also around CI Tau (Johns-Krull et al., 2016a), which is CTTS. However, the planetary status of the very-first short-periodic planet candidate orbiting CVSO 30 every 0.44 d on inclined orbit (van Eyken et al., 2012), is still uncertain and the subject of debate (Yu et al., 2015). Time-series H-alpha spectroscopy strongly suggests that this planet may be subject to tidal disruption, as it appears that it is losing its mass through the Roche lobe overflow mechanism (Johns-Krull et al., 2016b).

Encouraged by the discovery of the putative planet CVSO 30b, as well as our discovery of semi-periodic/random dips in 2011 *MOST* satellite observations of TW Hya, likely the results of hot spots occultations by dusty clumps (Siwak et al., 2014), we decided to conduct high-cadence (30-90 sec) multi-colour survey of pre-main sequence stars available from the northern hemisphere. The main goal was to deliver evidences for more similar phenomenons for further sophisticated studies.

Additional benefits of such high-cadence data sampling, uncommon for the major space-based photometric telescopes, is the ability for study of rapid accretion-induced effects occurring in the time scales as short as a few minutes. Photometric data obtained during irregularly distributed nights can also be used for rough characterisation of large-scale dips, caused by dusty disc warps and/or massive disc winds. These data are also well suited for determination of rotational periods – a basic “clock” in a star-disc system – which has still very high importance for a proper description of the overall spin-age relation for the pre-main sequence stars and is essential for our understanding of the rotation-braking process (Bouvier et al., 2014; Karim et al., 2016). Its later stages are now better understood: After roughly 5-10 Myr, when an accretion disc material is depleted and the star-disc locking mechanism can no longer operate, the former CTTS and now WTTS spins up due to conservation of its angular momentum during its contraction and falls into a region of 1-2 day periodicities. At this stage, hot accretion-induced spots no longer form and light curves are mainly modulated by stable cold spots, permitting even studies of differential surface rotation (e.g. Grankin et al., 2008; Siwak et al., 2011b).

Details of our Mount Suhora Observatory (*MSO*) observations are described in Section 2. Variety of results obtained during this survey are described and immediately discussed in Section 3. We summarize our main findings in Section 4.

2. Target selection, observations and data reduction

We compiled initial list of targets based on Herbig et al. (1994) and Grankin et al. (2007). As the time progressed, the list was slightly modified to increase efficiency of this survey: observations of fields containing a handful instead of only single or two young stars were preferred. Poor weather conditions during all but first Winter (2013/2014) of our survey nominal duration time forced us to skip observations of a few preselected fields from Taurus, Auriga and Orion constellations. Fortunately, most of these missed members of “Taurus-Auriga” Star Forming Region (SFR) was later observed during *Kepler-K2* mission (Borucki et al., 2010) and by *TESS* mission (Ricker et al., 2015) – results obtained by means of these space-telescopes are incomparably richer and will be the subject of separate publications. The list of all young stars (compiled from SIMBAD database) contained in 20 fields (column 1)¹ and bright enough for *MSO* telescopes is presented in column 2 in

¹These fields are numbered according to their observation start dates. Field #1 is centered on “R1 Mon” association, fields #4, 8, 10, 13 and 14 contain members of “Taurus-Auriga” SFR, field #2 includes most members of “Gulf-Mexico”, i.e. the small part of “North America” SFR, field #7 includes a fraction of “Pelican Nebulae” (IC 5070) SFR members, while field #9 members of NGC 6914 association. Targets from fields #5, 6, 11, 15, 16 and 19 were selected among members of “Cepheus-flare” SFR; more specifically fields #5 and 11 contain young stars forming in (and nearby) the famous NGC 7023 and NGC 7129 nebulae, respectively, while field #15 nearby L1261 cloud. BM And (field #3) is the only CTTS observed in “GAL 110-13” association, while V594 Cas is

Tables 1-4. Many of these stars were previously observed by other authors, who focused on investigation of long-term variability, determination of accretion diagnostics to estimate major stellar parameters, and also disc-related infrared fluxes. We do not present detailed time-ranked historical results for every individual target. Instead, in the next section we will shortly discuss our major achievements in the historical context only for a couple of stars, which show puzzling variability and were therefore more widely investigated in the past by other authors.

The vast majority of the *MSO* data was collected with the 60 cm Carl-Zeiss telescope. Originally in Cassegrain configuration, the telescope was later modified to operate in the primary focus for the purposes of M-dwarfs survey (Baran et al., 2011). Three CCD cameras and four photometric systems were utilized. Between March, 2012 – September, 2013, we used the SBIG ST10XME CCD camera equipped with the Johnson-Morgan filters provided by SBIG. In October, 2013, the Apogee Alta U42 CCD camera, equipped with a set of Johnson-Bessel filters manufactured by Custom Scientific was installed on the telescope. In August, 2014, we started to collect our data through Sloan filters, which have several advantages over the former filter sets: the pass bands of Sloan system are practically independent of each other, and transmission efficiency of every single filter is higher. At the time the Apogee ASPEN CG47 camera replaced the above one. Only for V395 Cep, which is about 10 magnitude bright star, the data were collected through Strömgren filters. Observations of five HAEBE stars, which are too bright for the 60-cm telescope, were obtained by means of the remotely operated 20-cm Ritchey-Chretien *MSO* telescope, equipped with SBIG ST10- XME CCD camera and the Johnson-Morgan filters provided by SBIG. We present detailed log of our observations in Tables 5-7.

In order to make a balance between information about colour indices, which is necessary to characterise mechanisms leading to specific light variations, and high cadence (30-90 sec) required for sufficient sampling of planetary transits and rapid accretion-induced events (Figure 1), most of our targets was observed in *BVI*, *VI*, *gi* or *gri* filters only. In order to find transits similar to CVSO 30, we made attempts to get full phase coverage for periods up to about 0.8 day. In practice, this requirement was met for most fields after 4-11 hours of continuous observations during 5-20 different nights (depending on the season), non-uniformly distributed over the time span of a few weeks. Fields containing particularly interesting targets were observed for one or two more seasons.

All frames were *bias*, *dark* and *flat-field* calibrated in a standard way within the MIDAS package (Warmels, 1991). Aperture photometry was obtained by means of C-MUNIPACK software (Motl, 2011) which utilizes DAOPHOT package (Stetson, 1987). As the weather conditions which are prevailing in Poland do not allow for frequent and accurate calibrations to the standard photometric systems, we de-

the only HAEBE from "RfN VDB 4" cloud. Field #12 show stars emerging from dusty "Serpens Molecular Cloud". None membership is known for the two HAEBEs from fields #17 and 18.

cided to left all data in instrumental systems. Light curves of all stars showing any variability occurring either in short, long, or in both time scales are shown in Figures 6-13². These light curves were also left uncorrected for the first and the second-order atmospheric extinction terms. However, using approximate colour extinction coefficients determined for *MSO*, we corrected the data used for calculation of colour-magnitude diagrams (Figs. 2,3,5) and phase-ordered observations in periodic stars (Fig. 4). We estimate that the uncertainties associated with inaccurate (up to 30%) determination of the color extinction values should not exceed 0.04 mag for stars having colour index redder/bluer than comparison star(s) by as much as 2 mag. The uncertainty should not exceed 0.01 mag for typical colour index difference of 0.5 mag. We note that these estimates relate to upper error values: they are calculated for $B - V$ and $g - r$ colour indices, which are most sensitive on innacurate colour extinction correction, and airmass 2 – the value which was rather exception than the rule during our observations.

Based on detailed visual inspection of the light curves shown in Figures 6-13, we have assigned our targets to one of the three major groups of variability, as indicated in column 3 in Tables 1-4. The group of "dippers" consists of stars observed close to the disc plane and their variability is owing to dusty disc warps, acting as occulting screens as they rotate around the star. Light curves of "accretors" are dominated, or at least occasionally affected, by chaotic hot spots created during inhomogeneous accretion. Finally, light curves of "periodic" stars are produced either by rotational modulation in visibiliy of persistent photospheric cold spots (in WTTS), or relatively stable hot spots (in CTTS), produced at the footprints of stable accretion funnel(s). We stress that classification given in this paper for stars previously not intensely observed by other authors do base on our sparse data only and may be the subject to changes, e.g. thanks to the ongoing *TESS* mission and long-term monitoring programs like *ROTOR* (Grankin et al., 2008) and that conducted at the Rozhen National Astronomical Observatory of Bulgaria (Ibryamov et al., 2014).

3. Results and discussion

3.1. The search for planetary-like transits

In the first step, we examined all light curves collected continuously for at least several hours for signatures of any brightness dips caused by transiting Jupiter-like planets or low-mass stellar companions, but with a negative result. Each light curve was examined several times: first immediately after the night, using preliminary set of comparison stars and later, during more detailed analyses using light curves received with final, more appropriate comparison stars (see in column 2 in Tables

²Only data obtained by means of the 60-cm telescope are shown – we decided to skip data gathered by means of the 20-cm telescope due to unstable *flat-field*. For the same reason, we omit the respective upper values of covered periods in Table 7

5-7). In these searches we based on estimates of Neuhauser et al. (2011) that young "inflated" planets having 1-10 Jupiter masses and orbiting typical T Tauri-type stars should produce 0.02-0.07 mag dips, which would be directly visible in our data. Even though it is a promising opportunity, we did not apply any automatic procedure for search for even more shallow transits. This is owing to numerous little ($\lesssim 0.005$ mag), accretion- and/or colour extinction-related variations (the latter caused by passing thin cirrus clouds), both leading to false-positive detections.

In the first column in Tables 5-7, just below the field numbers, we list the appropriate upper values of periods almost completely covered by our observations. We stress that single-site observations disabled us to get good phase coverage for periods equal to 0.5 ± 0.01 d. In addition, only limited amount of stars (see in the second column in Tables 1-4), for which photometric quality of 1% of single observational points was achieved, is suitable for detection of 1-5% transit-like dips. As the vast majority of our targets are M-K type dwarfs, which are often additionally heavily reddened by dusty environments, in many cases search for the transits was only possible in light curves obtained in *i*-bands. This band is also least "polluted" by hot spots, which decrease amplitude of potential transits. Finally, the light curves gathered for targets 1.5-2 mag fainter than mean (artificial) comparison star were usually suitable only for studies of large-amplitude light variations.

3.2. Accretors

Most of our targets belong to CTTS, which are constantly transferring disc plasma in unstable regime or just show episodes of inhomogeneous accretion. Although space-based uninterrupted light curves are best suited for investigation of these phenomena, time-coherent variability caused by accretion can sometimes be as short as 10-30 min and can be still successfully investigated from the ground (Gullbring et al., 1996; Siwak et al., 2018).

Stars in which accretion effects dominate in overall brightness variations are indicated in the third column in Tables 1-4 as "accretors". We also include into this group several stars showing smooth brightness variations for most of the time, but interrupted by several well-defined "accretion bursts" (Fig. 1 a,b,c,d). These bursts are of triangular shape and can be well distinguished from other rapid brightness variations, e.g. stellar flares. As mentioned above, due to the temperature contrast between typical hot spot ($\sim 5000 - 10000$ K) and photosphere (~ 4000 K), the largest amplitudes of these light variations are observed in the blue part of the spectrum and decrease towards longer wavelengths. This dependence is true both for large-scale and small-scale accretion-induced variability.

Siwak et al. (2018) showed that time-coherent variability in TW Hya mimicking oscillatory behavior can be as short as 10-30 min. Only one star from our sample, namely FU Cep, is in many aspects similar to TW Hya: its 2014 observations (Fig.1c) showed two single accretion bursts of the duration times 33 min (at $HJD = 2456958.331$) and 56 min (at $HJD = 2456960.430$), respectively. But

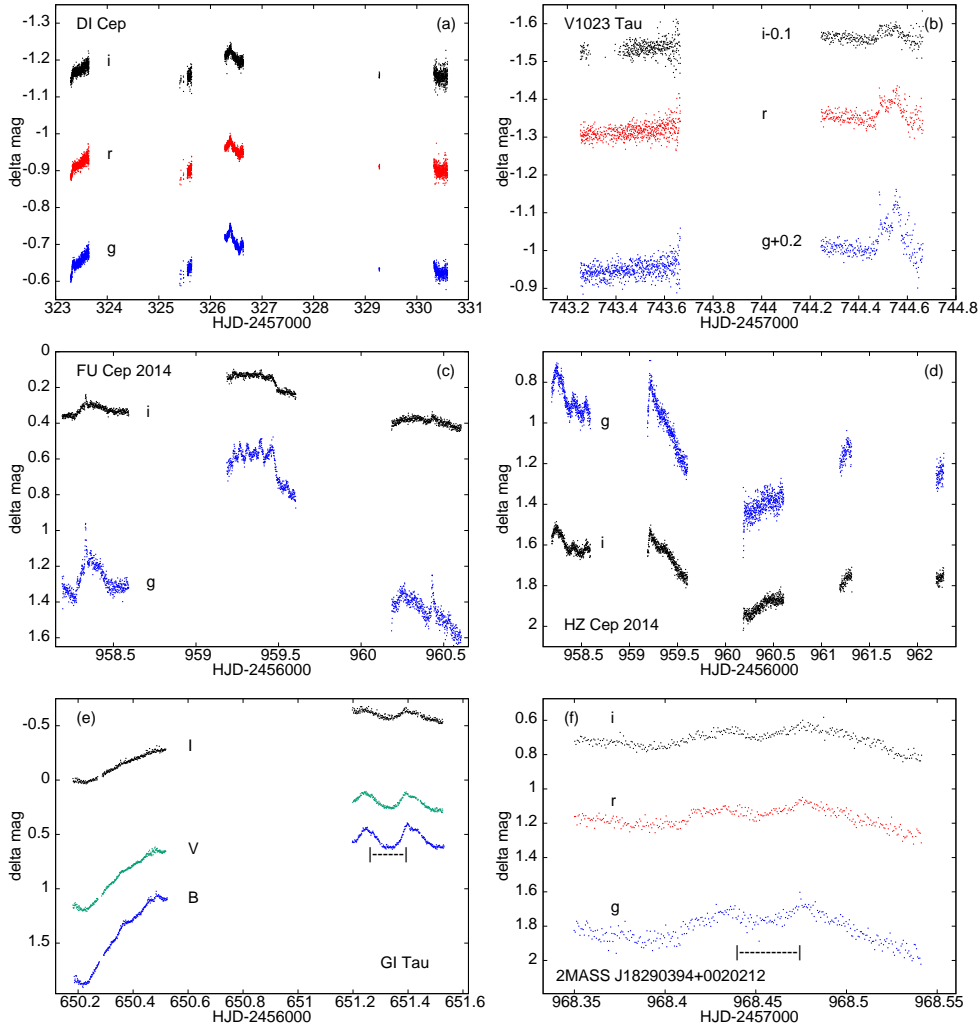


Fig. 1. Light curves of six stars classified as accretors. The best defined oscillatory behavior, with the characteristic period of 56.4 min, is visible in the local maximum of FU Cep, but single flare-like accretion bursts are also present during other nights. The two bottom panels show possible occultations of hot spots during the local brightness maxima of two stars, as indicated by marks.

the most intriguing finding is the oscillatory behavior during the local brightness maximum at $HJD \approx 2456959.35$, lasting for the entire maximum plateau. To calculate their period first we removed small trend in the maximum using low-order polynomial and then we transformed the data to flux units. We obtained frequency spectrum which shows single well-defined peak at 56.4 min. Interestingly, it is similar in terms of duration to the second aforementioned accretion burst (at $HJD = 2456960.430$). We have preliminarily proposed to explain these oscillations in TW Hya as caused by post-shock plasma oscillations. This conclusion was based on the theoretical result of Matsakos et al. (2013), who presented a range of models, among them one with an oblique impacting surface leading to QPO of

15 min. However, the period found in FU Cep is almost four times longer. Similarity of the second single accretion burst duration time and these oscillations period (56 min) gives hint that perhaps other hypothetical scenario (already also considered by us for TW Hya) can more plausibly explain observed phenomenon: one can not exclude the possibility that for some reason small plasma clumps hit the star at regular intervals, what mimics oscillatory behavior. Theoretical models of this phenomenon are strongly desirable.

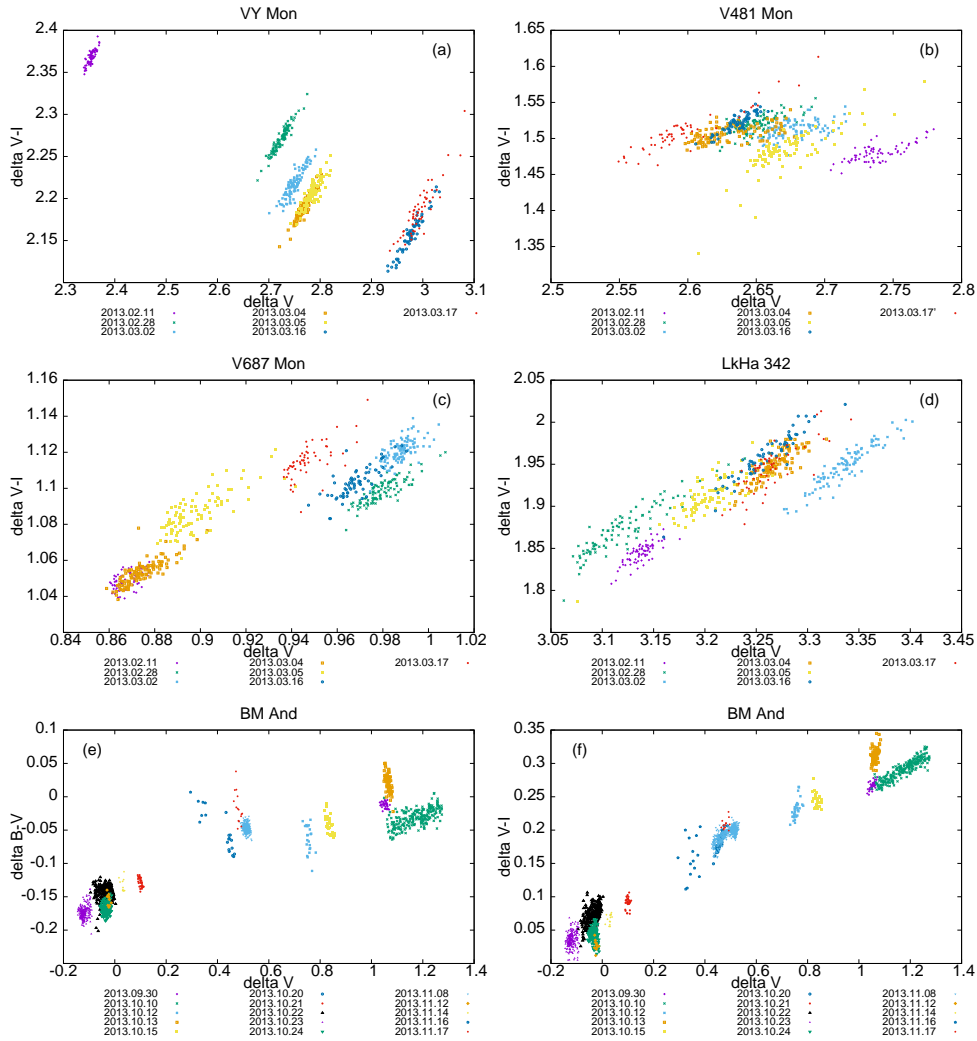


Fig. 2. Colour-magnitude diagrams for VY Mon, V481 Mon, V687 Mon, LkHa 342 and BM And. Data obtained during different nights are marked with different symbols and colours (see legends below respective x-axes). Only data obtained by means of SBIG camera and filters were used to construct diagrams for the first four stars. Whilst the general trends observed in these diagrams are intrinsic to the stars, the intra-night and the night-to-night scatter visible in diagrams of first four stars may also be related with uncertainty in our colour extinction correction procedure to some extent (see in Section 2).

3.3. Dippers

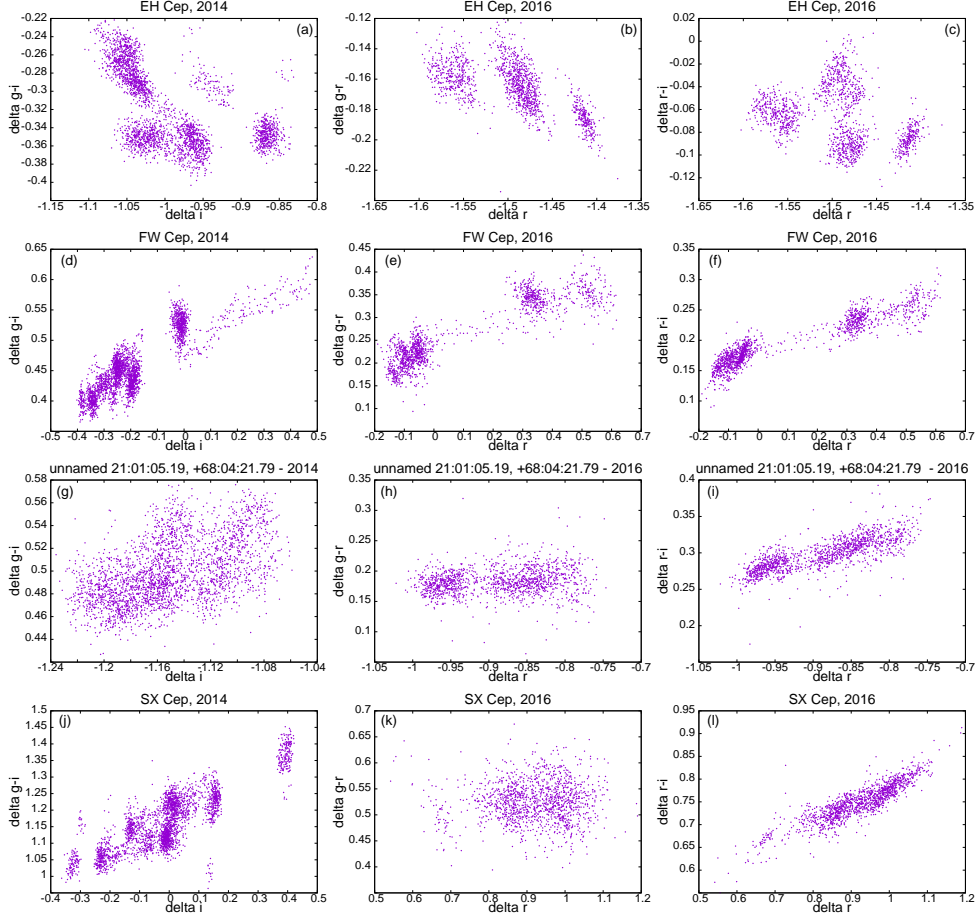


Fig. 3. Colour-magnitude diagrams for EH Cep, FW Cep, the unnamed CTTS-candidate and SX Cep. While colours of the last three star are becoming redder when the stars are fainter, it appears to be not the case for EH Cep.

The characteristic feature of "dippers" are regular or semi-regular large brightness drops (e.g. Bouvier et al., 2003). The unified models of this phenomenon were most recently presented by McGinnis et al. (2015) and Bodman et al. (2017). Based on analysis of consecutive occultations observed by *CoRoT* spacecraft in a dozen of dippers in NGC 2264 SFR and by *Kepler-K2* in Upper Sco SFR, the authors obtained that the maximum warp height over the disc plane amounts to about 20-30 per cent of the disc radius at which it originates, and that it may vary by 10-20 per cent on a time-scale of days. It is normally assumed that the major warp causing partial or total occultations of stars arises as the result of star-disc interaction through magnetic field (Romanova et al., 2013). The optical thickness of the associated funnel flow is subject to change for external observer, depending on elongation over the disc plane. Similar level of light drop during given minimum

observed in all bands indicates that warp is composed of grains larger than $1\mu\text{m}$ (Bouvier et al., 1999).

Particularly interesting objects of this type, which were previously studied by other authors, were also observed at the *MSO*. They are as follows:

- VY Mon is the most studied star among those observed in field #1. It is Herbig Ae/Be star and according to Miroschnischenko et al. (1992) the star was also strongly variable in the past (at 1.5 mag in Johnson *V*-filter) but the variability scale is strongly increased toward shorter wavelengths. H-alpha line profiles are variable between P-Cygni type and a single peak, what suggests that high-velocity outflows can be important envelope components (Pavlova et al., 2005); this view may be particularly true if one takes into account very high mass accretion rate of $10^{-4} M_{\odot} \text{yr}^{-1}$ (Mendigutia et al., 2012). This is probably the youngest star investigated here, as its age derived from position on H-R diagram and theoretical evolutionary track of pre-main sequence stars does not cross 10^4 years (Manoj et al., 2006). Our data gathered for this star are presented in Fig. 6g. The colour-magnitude diagram (Fig. 2a) shows unusual trend: the star is becoming bluer when the brightness decreases, what is not observed in other dippers in this field (Fig. 2b,c,d), nor for BM And (Fig. 2e,f). In stars showing significant light variations due to variable extinction and without signatures of hot spots any search for rotational period is doomed to failure, as in our case.
- V521 Cyg appears to be the only "dipper" among the stars from field #2. The star was frequently observed in current decade due to close vicinity to one of the most recent FU Ori-type star (FUor) V2493 Cyg (Semkov et al., 2010). According to Poljancic Beljan et al. (2014) and Ibryamov et al. (2015, 2016) the major dips in V521 Cyg can be folded with the period 503 d. Although our observations considerably overlap with the data gathered by these authors, we did not observe any of these large-scale dips at the *MSO* – only secondary though considerable (1 mag in *V*-filter) light drop at $HJD \approx 2456580$ was noticed (Fig. 7a). For the rest of the time the star remained in high brightness state and showed only little light variations. Our attempts to search for periodic signals during the light "plateau" have failed.
- BM And is the only young star observed in field #3. In the agreement with historical results, our data indicate on large variations (Fig. 7n) due to variable extinction, most probably caused by large grains contained in the disc warps (Walker, 1980). According to Grinin et al. (1995) the star is observed edge-on. It shows typical behaviour as AA Tau, i.e. it becomes redder when fainter (Fig. 2e,f).
- Field #5 turned out to be most interesting region monitored during our survey. According to Grankin et al. (2007) the blue turnaround of colour-magnitude

diagrams at minimum brightness of EH Cep suggests light scattering (most efficient in blue band) by circumstellar extinction: as the stellar photosphere is partly occulted by circumstellar material (most likely the disc wind), the ratio of scattered light to direct light increases, and the system becomes bluer. This mechanism could potentially explain, why the range of light variations in EH Cep observed during our survey is smaller in g' -band than in r' and i' bands (Fig. 8a,b). We stress, that this behavior appears to be always visible in EH Cep (Fig. 3a,b,c), regardless of the brightness of this star. Note that this effect was previously observed by us even more clearly in VY Mon, where massive outflow in the form of disc wind is the rule.

- FW Cep is classified as CTTS (Kun et al., 2009). Although our monitoring in 2014 and 2016 was relatively short, our data show well-defined brightness dips, with the decline and rise times of a few hours (Fig. 8e,f). The colour-magnitude diagrams show trends typical for AA Tau-like stars (Fig. 3d,e,f).
- Similar well-defined dips were observed almost every single night in the bright star from field #5, which remains unnamed in SIMBAD database, localised at $\alpha_{ICRS\ 2000} = 21^h01^m05.19^s$, $\delta_{ICRS\ 2000} = 68^\circ04'21.79''$ (Fig. 9m,n). Nevertheless, we decided to present photometry of this star as it shows X-ray and infrared excesses typical for other CTTS. So far we were only able to establish that colour-magnitude diagrams of this star show behaviour typical for "dippers" (Fig. 3g,h,i).

3.4. The search for short-term, small-scale TW Hya light dips

In addition to "dippers" showing light drops as large as 1-3 mag, Siwak et al. (2014) reported *MOST* satellite discovery of semi-regular shallow ($\sim 0.02 - 0.03$ mag) dips in TW Hya. Intense monitoring of this star both with the *MOST* satellite and from the ground showed that the high occultation frequency seen in 2011 was rather exception than the rule (Siwak et al., 2018). We obtained that these dips do occur only in some local brightness maxima and are likely caused by occultations of hot spots by: (1) total or partial absorption of their light by condensed dusty clumps carried toward the star within associated accretion tongue, or (2) total or partial absorption of their light by the plasma carried toward the star within associated accretion tongue, which becomes optically-thick in $U\&B$ -filters. The search for similar events in other CTTS to better establish mechanisms leading to this phenomenon was one of the main driving forces leading us to undertake this survey. As their branch duration times in TW Hya were of the order of 1-2 min, and the total duration times were of 10-20 min we decided to fit single filter change cycle in 30-90 sec, depending on stars brightnesses.

Careful inspection all *MSO* data obtained for "accretors" reveal only two possibilities of such events: the first was seen in the light curve of GI Tau, at $HJD = 2456651.33$ and the second in 2MASS J18290394+0020212 (Figure 1e,f). The

low detection rate is in line with the results for TW Hya, but the event in GI Tau lasted remarkably long: the total duration amounted to almost 3.5 h, but the total flat minimum lasted almost 1.1 h. In the second case, the respective duration times were significantly shorter, 0.91 h, and 0.36 hr. Negative detection of dips lasting for 10-20 min, as in our discovery data in TW Hya, may either suggests that these are extremely rare events, or that they remained undetected because of relatively small effective coverage time of every field. This search may perhaps be worth of resume in the future, when massive space-based continuous monitoring of the large parts of the sky in at least two bands (e.g. Pigulski et al., 2017) will become the rule.

3.5. *Periodic stars*

Data obtained during randomly distributed nights over a few weeks, months, or even during different seasons, may allow to determine rotational periods of stars if they posses stable spots. This can be easily accomplished for WTTS, whose light curves are modulated by persistent cold spots (Grankin et al., 2008), and for CTTS accreting in the stable and the moderately stable regime, which creates two antipodal hot spots (e.g. Herbst et al., 1994; Siwak et al., 2016). Nevertheless, this regular variability pattern seen in CTTS can sometimes be disturbed by fractional or total occultation of central star by warps in the discs (e.g. SU Aur Cody et al., 2013; Grankin et al., 2018), or by pulsed accretion (Tofflemire et al., 2017a, 2017b; Biddle et al., 2018), what significantly limits potential of ground-based data for searches for stable periods.

We performed frequency analysis using the method described in Rucinski et al. (2008). Surprisingly, in spite of large number of monitored stars regular variability patterns turned out to be rather uncommon: only seven periodic stars was found in "Gulf-Mexico" SFR (field #2) and another single star was found in field #15.

Three out of seven periodic stars from "Gulf-Mexico" SFR were previously known to show regular variations: we confirmed the value of short period for the CTTS star V1716 Cyg at 4.16 ± 0.09 d (ver. 4.1539 ± 0.0002 d in Poljancic Beljan et al., 2014) and for likely WTTS star V1929 Cyg at 0.4263 ± 0.0015 d (ver. 0.426257 ± 0.000306 d given by Ibryamov et al., 2015). In line with these authors we also obtained the period of 2.42 ± 0.05 d for LkHa 189, which is probably CTTS. Contrary to Ibryamov et al. (2015), we found stable period for V1957 Cyg at 5.2875 ± 0.0080 d, yet, the author argue that it may be field M0V dwarf, rather than WTTS. Except of the above, we also found periodic signals for 2MASS J20580604 +4349328 (at 1.333 ± 0.010 d), 2MASS J20580885+4346598 (5.85 ± 0.01 d) and the very short 0.3692 ± 0.0015 d well-defined variations in the visual component of the likely visual binary star [RGS2011] J205745.44 +434845.1. All these three stars are classified as young stellar objects in SIMBAD database, are well-visible on X-ray and infrared images, yet, the short 0.37 d period of the last star strongly suggests that it may be WTTS. Spectroscopic observations of this star are strongly encouraged. If the WTTS membership is confirmed, it would be one of the fastest

rotating WTTS ever observed.

We also note that neither our nor Ibraymov et al. (2015, 2016) data do not confirm the period of 2.08 d for LkHa 191, reported by Artemenko et al. (2012). Interestingly, in spite of stable behavior of V1716 Cyg in our data set (see above), Findestein et al. (2013) classified this star as a burster: the first event of inhomogeneous accretion lasted 5-20 days while the second was found 35 days later and lasted for about 3 days.

The last star among our targets showing regular variations is V395 Cep, also known as AS 507 and BD +73 1031. It is classified as CTTS with the moderate value of the mass accretion rate $3 \times 10^{-9} \text{ M}_{\odot} \text{ yr}^{-1}$ (Kun et al., 2009; Frasca et al., 2018). It was previously found as periodic star (at 3.432 d) by Chugainov et al. (1995) and our data phased with this value fully support their result. Stability of this value since almost three decades indicates that it is strictly related with stellar rotation, most probably with a hot spot produced by stable funnel flow. Similar long-term stable modulation was also noticed for IM Lupi (Siwak et al., 2016) and for SU Aur (Cody et al., 2013).

We also noticed slight excesses of power in frequency spectra of a handful of other young stars from fields #7 and #9, but data phased with respective periods do not show any regular patterns. Among them are LkHa 168 and LkHa 172 observed by Ibraymov et al. (2018), who were also unable to find any periodic behavior. These and other similar stars showing little but eventually false-positive signatures of periodic behaviour are usually classified as HAEBE or partly embedded young stellar objects (YSO). We stress that even the precise *MOST* satellite observations of HD 37806 and AB Aur did not firmly reveal any periodic variability (Rucinski et al., 2010; Cody et al., 2013). In addition, although the light curves appear to be similar to these of CTTS, amplitudes of light variations are considerably scaled down, to the level impossible for detailed investigation from the ground.

3.6. Stars with uncertain causes of variability

As mentioned above, many stars classified as YSO and HAEBE exhibit amplitudes of brightness changes too small to be detailedly investigated from the ground. This is in accord with Herbst & Shevchenko (1999), who stated that HAEBE often show little and (mostly) irregular variations beyond the major flux dips (if any), which are occurring in long time scales. They conclude, that these stars evidently do not possess either the large, stable cool spots or persistent hot spots associated with strong surface magnetic fields and magnetospheric accretion mechanism, which is the rule for CTTS.

Except of these stars, we observed several stars with considerable light variations and yet the exact mechanism leading to these light changes remains unknown:

- SX Cep and 2MASS J21014358+6809361 (field #5) are classified as WTTS (Kun et al., 2009) and show significant variations in time scales of hours and days. The second star showed also one stellar flare during the 2016

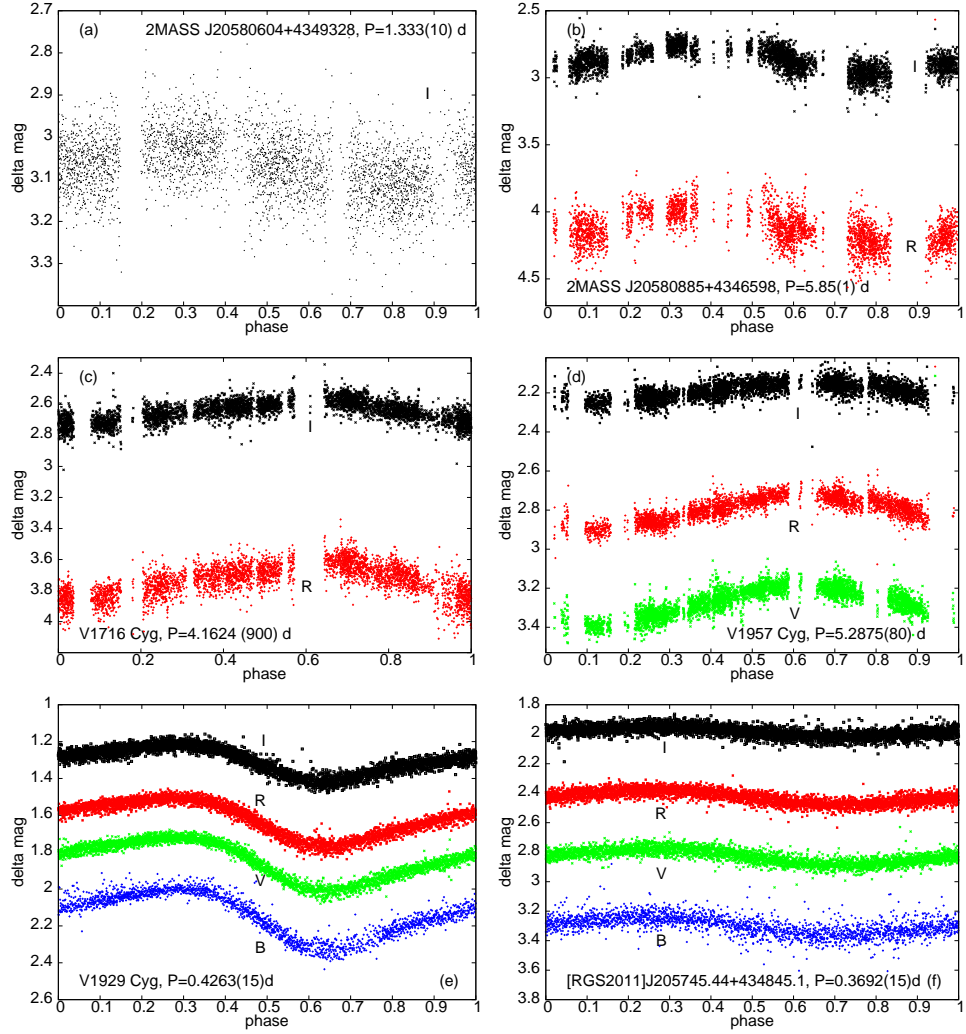


Fig. 4. Periodic T Tauri-type stars in "Gulf-Mexico" SFR.

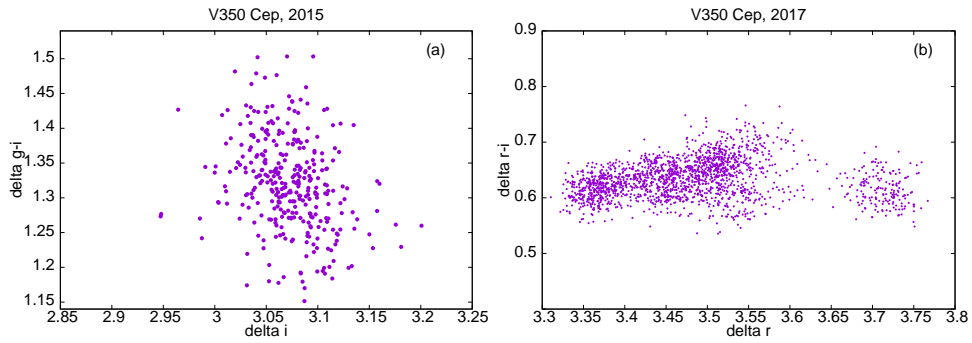


Fig. 5. Colour-magnitude diagrams for V350 Cep.

run (Fig. 9j). However, we failed to find any stable periods both in separate and combined 2014 and 2016 data sets. The colour-magnitude diagrams of both stars (see in Fig. 3j,k,l for SX Cep) show similar amplitudes of light variations in g and r filters. This may suggest presence of hot spot(s) with a temperature only slightly higher than the temperature of the photosphere, similarly as for MN Lup (Strassmeier et al., 2005). If it is the case, perhaps CTTS classification would be more appropriate for these stars.

- Variability of 2MASS J21012706+6810381 and 2MASS J21011252+6810-195 from the same field may appear to be due to variable extinction, but our data are insufficient to confirm this view – stellar rotation with hot spots may also be responsible for observed pattern. For the same reason, we are unable to conclude what is the mechanism leading to variability in LkHa 428, where we observe combined light of two components of this young wide binary star.
- V350 Cep was preliminarily classified as EXor or FUor (Ibryamov et al., 2014), but this was later put in doubts by Dahm et al. (2015) and Jurdana-Sepic et al. (2018). The last authors classified it as "dipper", but also this classification was later questioned by Semkov et al. (2017). Data gathered during our survey are too poor to resolve this ambiguity. The colour-magnitude diagrams constructed from all available data do not show any significant trends (Fig. 5a,b).

4. Summary

We performed the first high-cadence survey of pre-main sequence stars dedicated to study variety of rapid light variations simultaneously in at least two visual bands³. Although we did not find any signs of planetary transits, the data proved to be useful for determination of rotational periods of some stars and for studies of mechanisms causing observed light variations. The most important findings are as follows:

- We determined rotational periods for four new stars in "Gulf-Mexico" SFR and confirmed the period stability in V395 Cep, i.e. that value determined more than two decades ago (Chugainov et al., 1995) is strictly related to the rotational period of the star.
- We found FU Cep to be one of the most intriguing accretors in our sample, as it showed rare event of oscillatory-like behavior in the local maximum, similar as TW Hya (Siwak et al., 2018). These oscillations were only seen in the blue band and arose right with the appearance of the hot spot causing

³Questions regarding this manuscript and requests for presented light curves and/or calibrated frames for independent measurements can be send to the first author of this paper at any time.

associated light maximum. We do not indicate any particular mechanism that could firmly explain this variability, but rather urge theorists to undertake theoretical studies of this issue (see e.g. de Sá et al., 2019).

- Most of our targets firmly classified as "dippers" show nearly "achromatic" variability, i.e. most likely caused by large grains, as in AA Tau (Bouvier et al., 1999). These stars are usually getting bluer when their brightness increases. Yet, EH Cep and VY Mon show inverse relationships – they are becoming bluer when their brightness decreases. This indicates significant radiation scattering (most efficient on short wavelengths) when the stars are obscured likely by disc wind, consisting of individual atoms and molecules rather than dusty grains.

Analysis of the *MSO* data gathered during this survey is not complete yet. We do not present here the results obtained for about 80 CTTS in young cluster IC 348, which will be the subject of separate publication. Similarly, our data obtained for two FUors will be analysed together with *TESS* light curves gathered during Cycle 2. Certainly, the massive inflow of uninterrupted light curves gathered by this satellite for huge amount of young stars may also reveal planetary transits, perhaps similar to CVSO 30b, the phenomenon strongly desired but undetected during our modest survey. We stress that despite the fact that *TESS* observations may sharpen the view on mechanisms causing variability in the aforementioned stars, it is limited to members of rather close and uncrowded star forming regions. Therefore ground-based monitoring is still mandatory for investigation of crowded fields, like these in Cygnus and Cepheus constellations.

Acknowledgements. The authors acknowledge Polish National Science Centre for two grants supporting this research: 2012/05/E/ST9/03915 (MS, MD, KG, WO, MW) and 2011/03/D/ST9/01808 (GS). This research has made use of the SIMBAD database, operated at CDS, Strasbourg, France. Special thanks are due prof. Stanislaw Zola and dr. Pawel Zielinski for taking short series of the data on a few occasions.

REFERENCES

- Alencar, S. H. P., Teixeira, P. S., Guimaraes, M. M., McGinnis, P. T., et al. 2010, *J*, **A&A**, 519.88
 Ansdell, M., Gaidos, E., Rappaport, S. A., Jacobs, T. L., et al. 2016, *ApJ*, **816**, 69.
 Artemenko, S. A.; Grankin, K. N.; Petrov, P. P. 2012, *AstL*, **38**, 783.
 Baran, A. S., Winiarski, M., Krzesinski, J., Fox-Machado, L., et al. 2011, *AcA*, **61**, 37.
 Benisty, M., Juhasz, A., Boccaletti, A., Avenhaus, H., Milli, J., et al. 2015, *A&A*, **578**, 6.
 Biddle, L. I., Johns-Krull, C.M., Llama, J., Prato, L., Skiff, B. A. 2018, *ApJL*, **853**, 2.
 Bodman, E. H. L., Quillen, A. C., Ansdell, M., Hippke, M., Boyajian, T. S. 2017, *MNRAS*, **470**, 202.
 Bouvier, J., Chelli, A., Allain, S., Carrasco, L., et al. 1999, *A&A*, **349**, 619.
 Bouvier, J., Grankin, K. N., Alencar, S. H. P., Dougados, C., et al. 2003, *A&A*, **409**, 169.

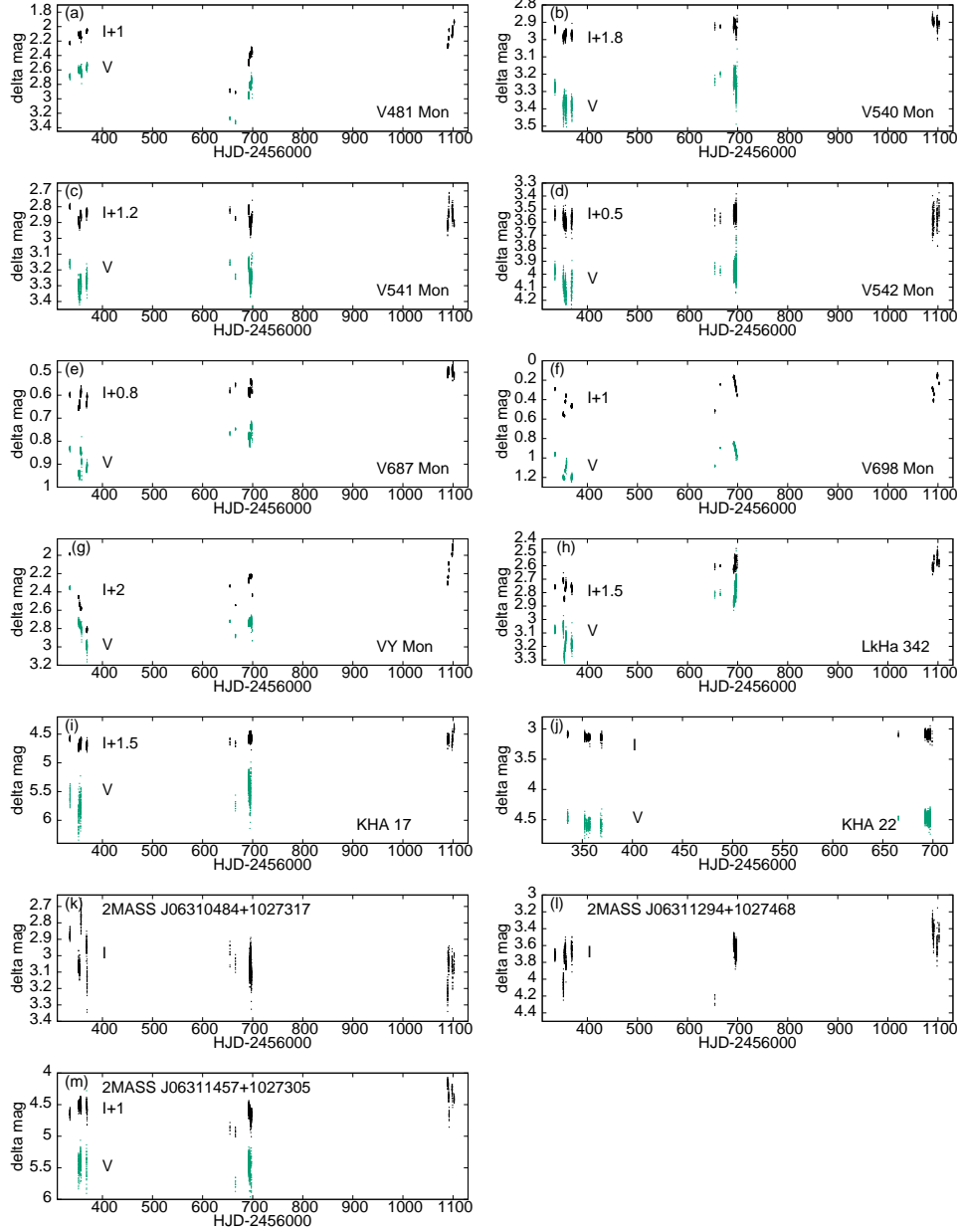


Fig. 6. Results of 2013, 2014 and 2015 runs for variable stars from field #1. Observations in V-filter were obtained during the first two seasons only. In addition, extraction of photometry in this band was impossible during nights with poor seeing conditions and/or bright Moon. Only data for stars, which evidently show any kind of variability, are shown.

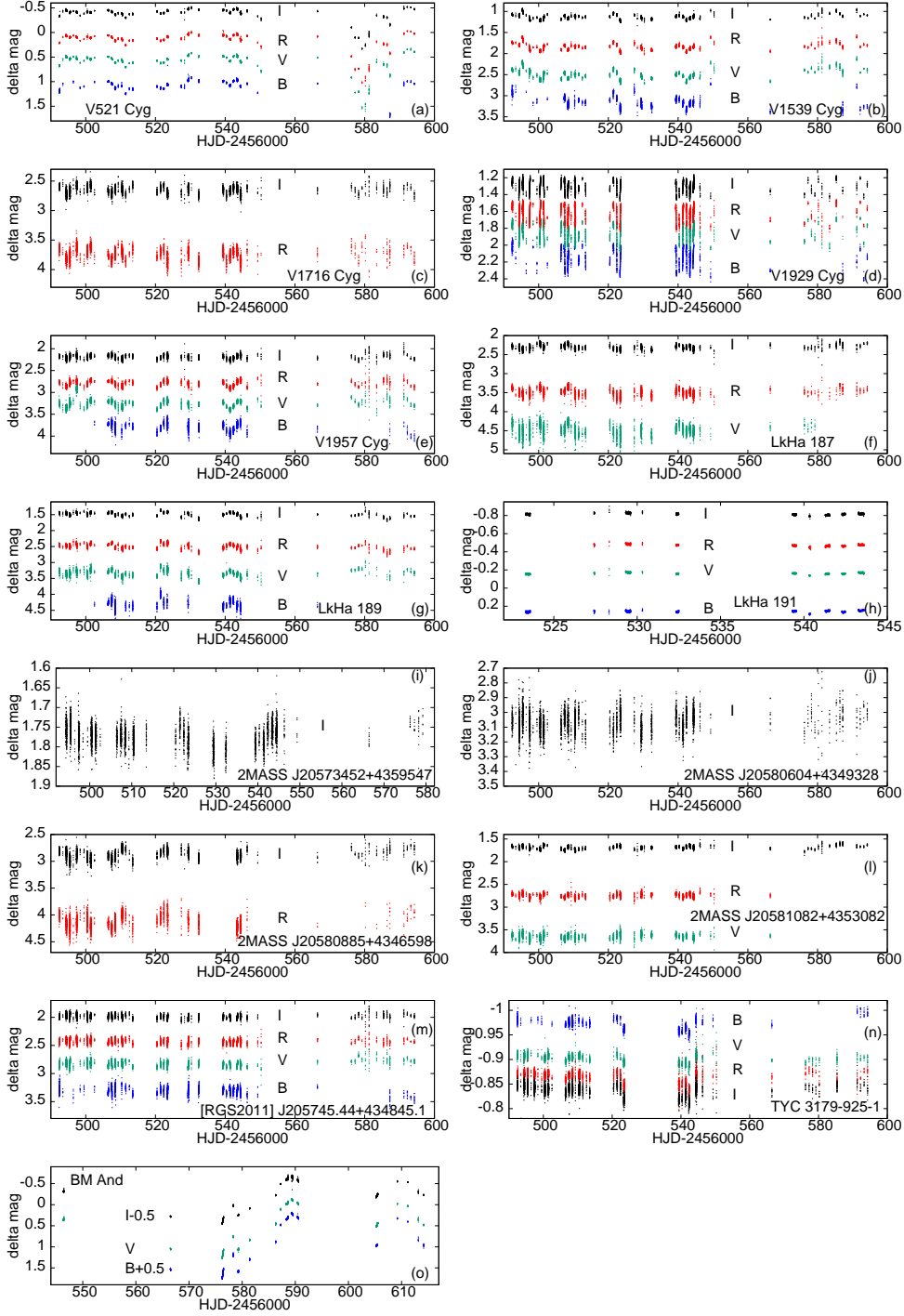


Fig. 7. Results for young variable stars from field #2 ("Gulf Mexico") and BM And (field #3).

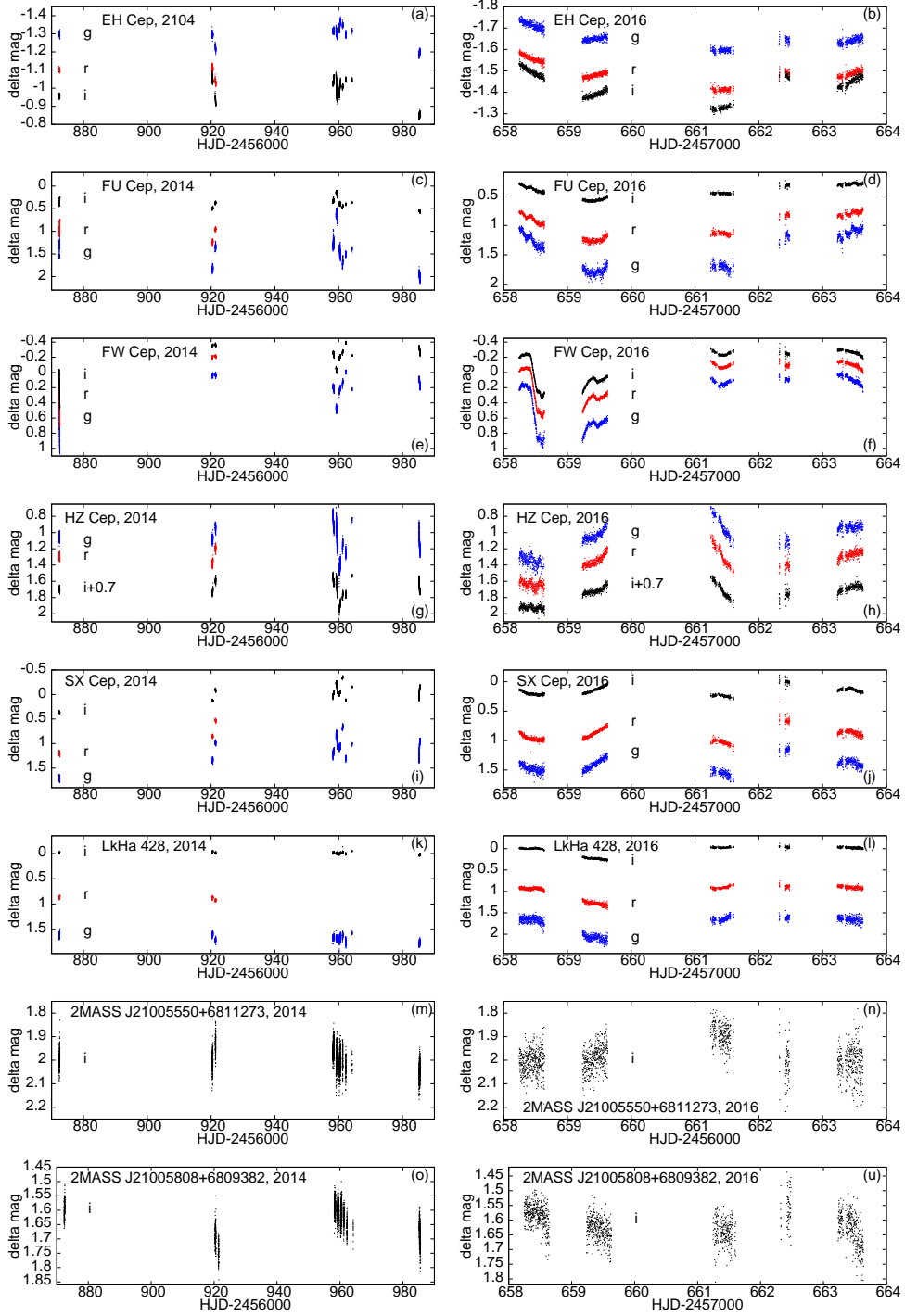


Fig. 8. Results of 2014 and 2016 observations of young variable stars from field #5 (NGC 7023).

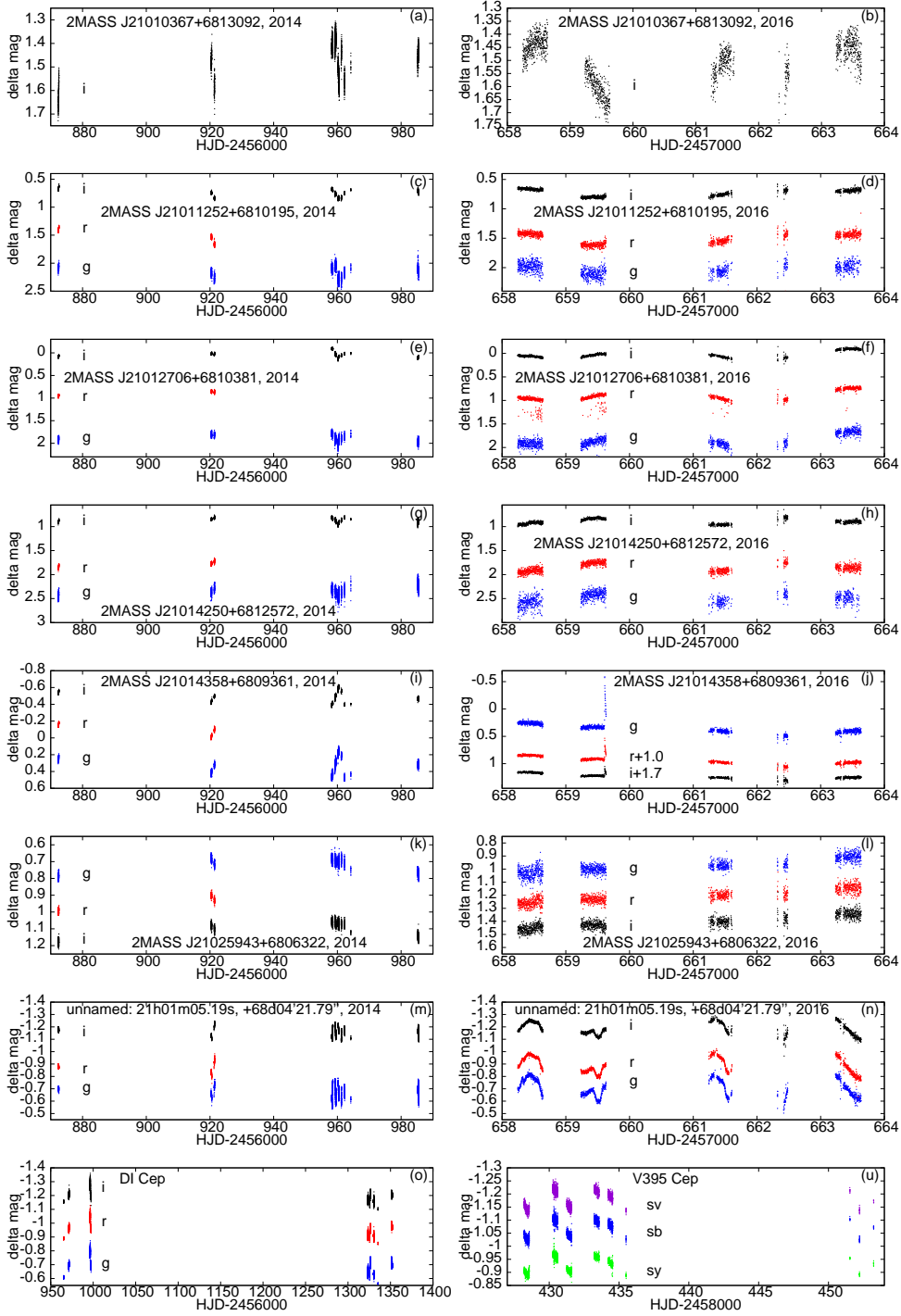


Fig. 9. Results of 2014 and 2016 observations of young variable stars from fields #5 (NGC 7023), #6 (DI Cep), and 2018 observations of V395 Cep (field #15).

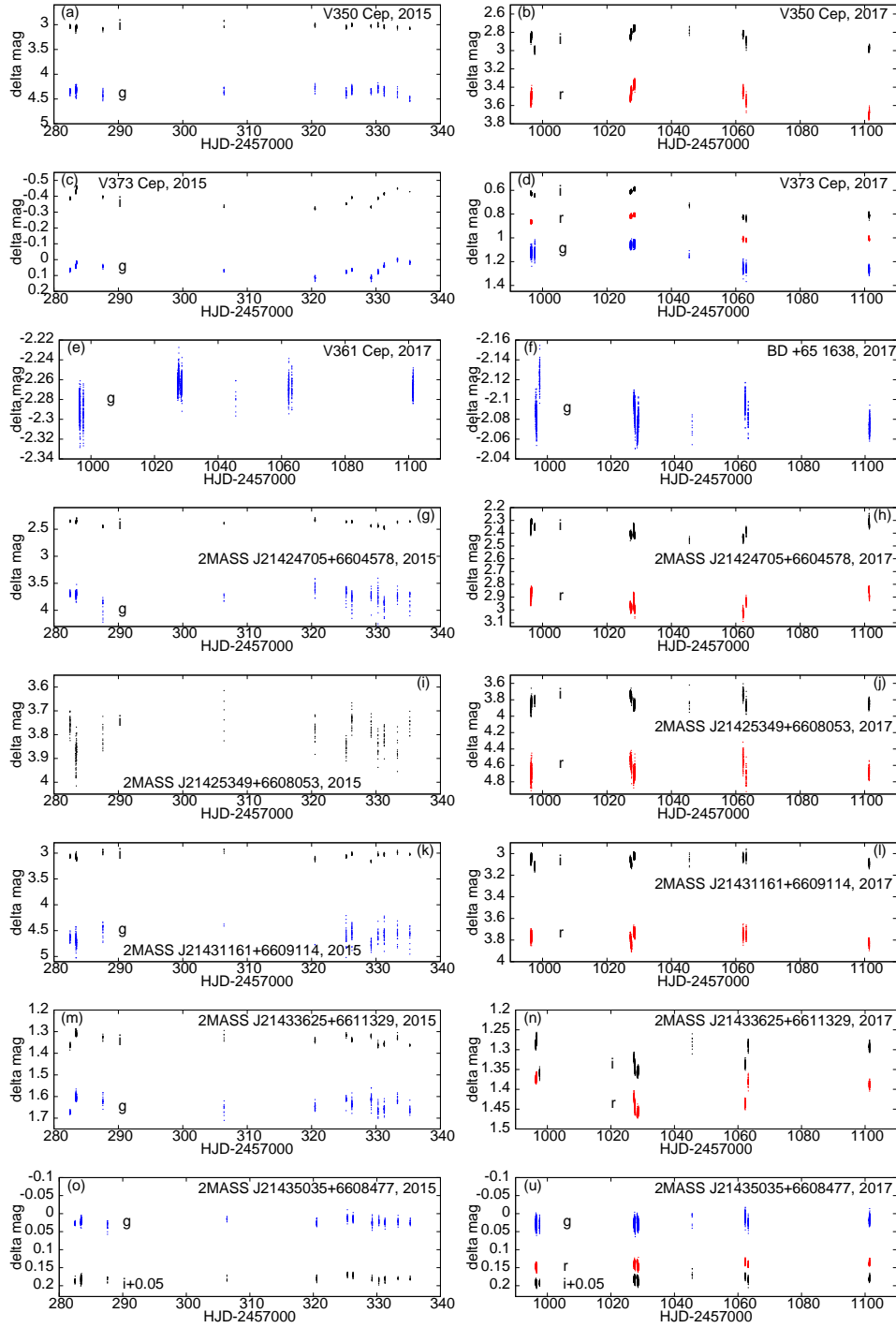


Fig. 10. Results of 2015 and 2017 observations of young variable stars from field #11 (NGC 7129).

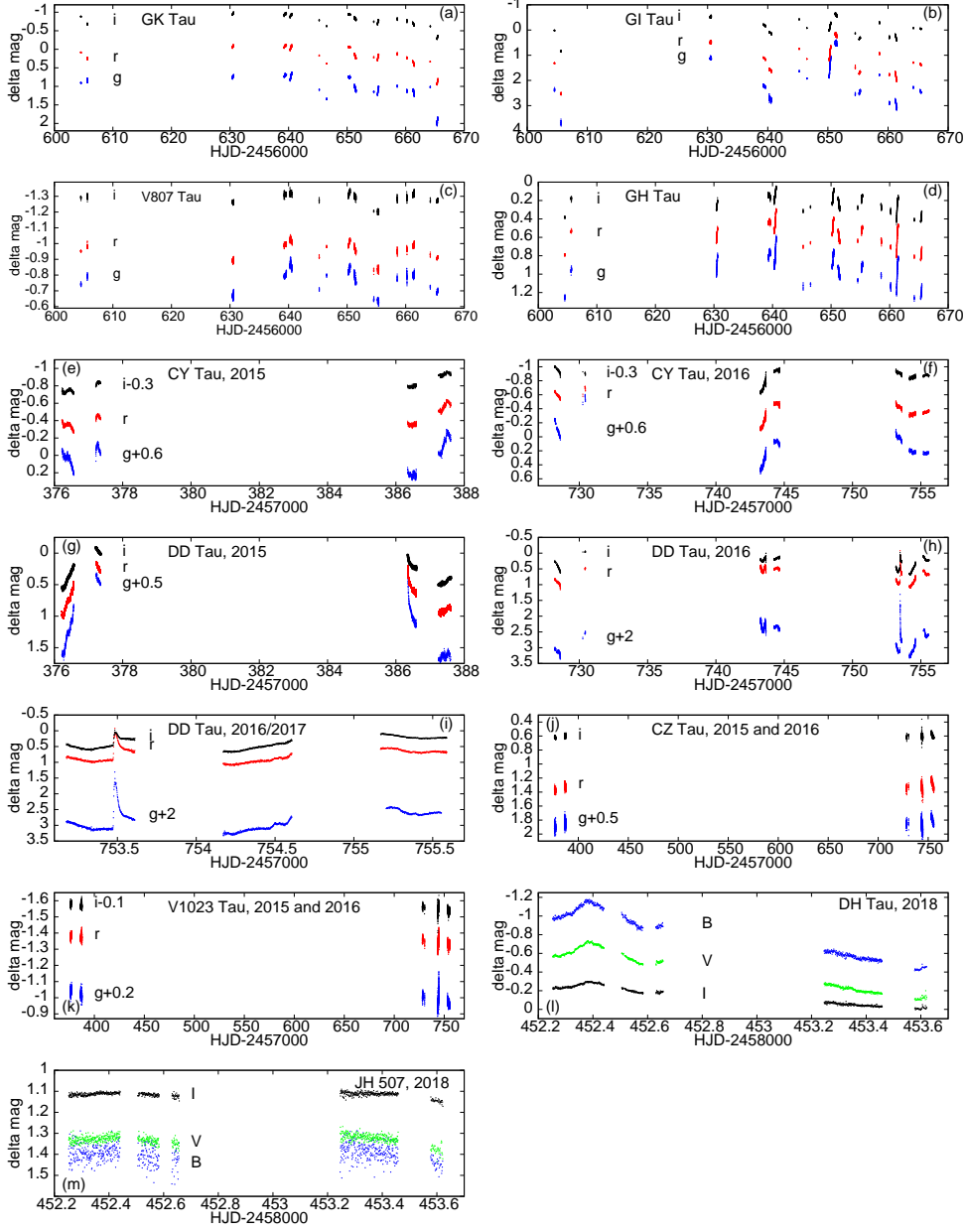


Fig. 11. Results for young variable stars from fields #4, #8, and #14 in "Taurus-Auriga" SFR.

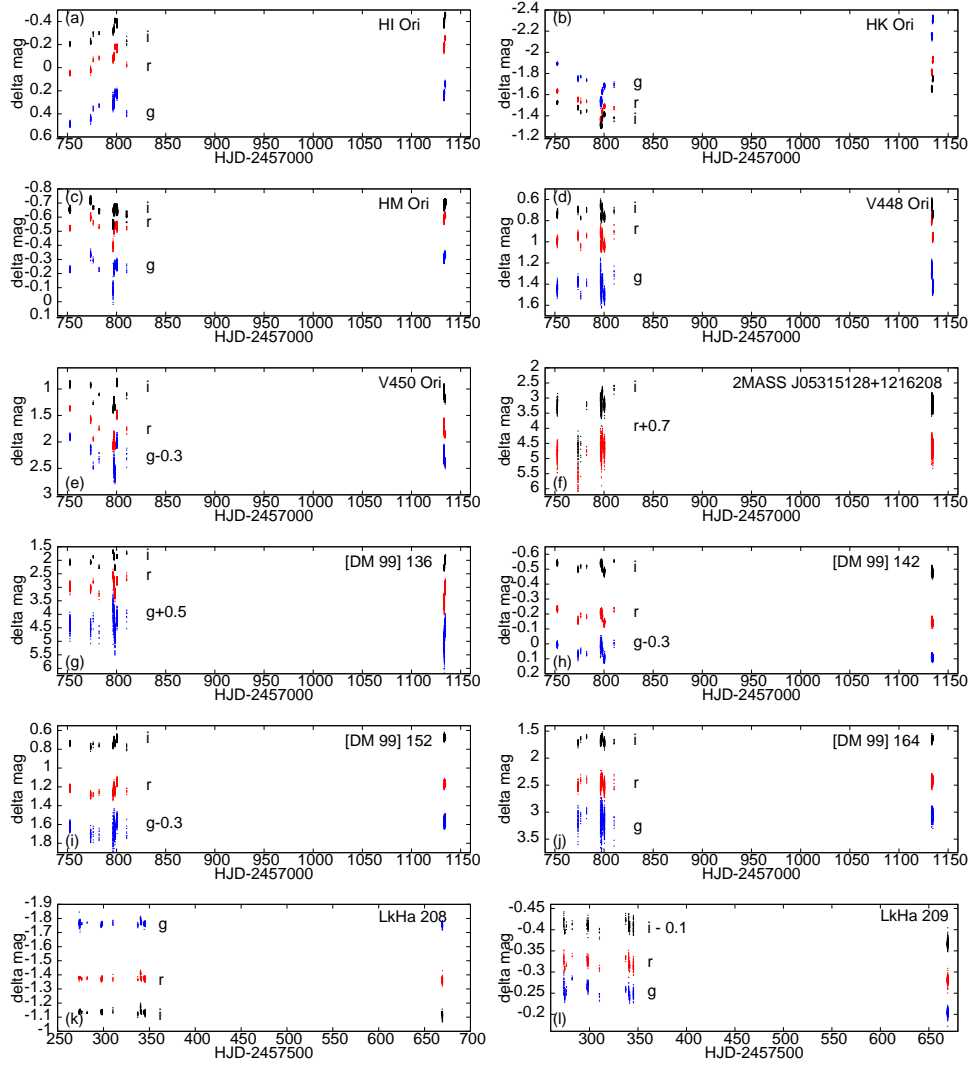


Fig. 12. Results for young variable stars from field #10 in "Taurus-Auriga" SFR. The last two panels show results for variables from field #13.

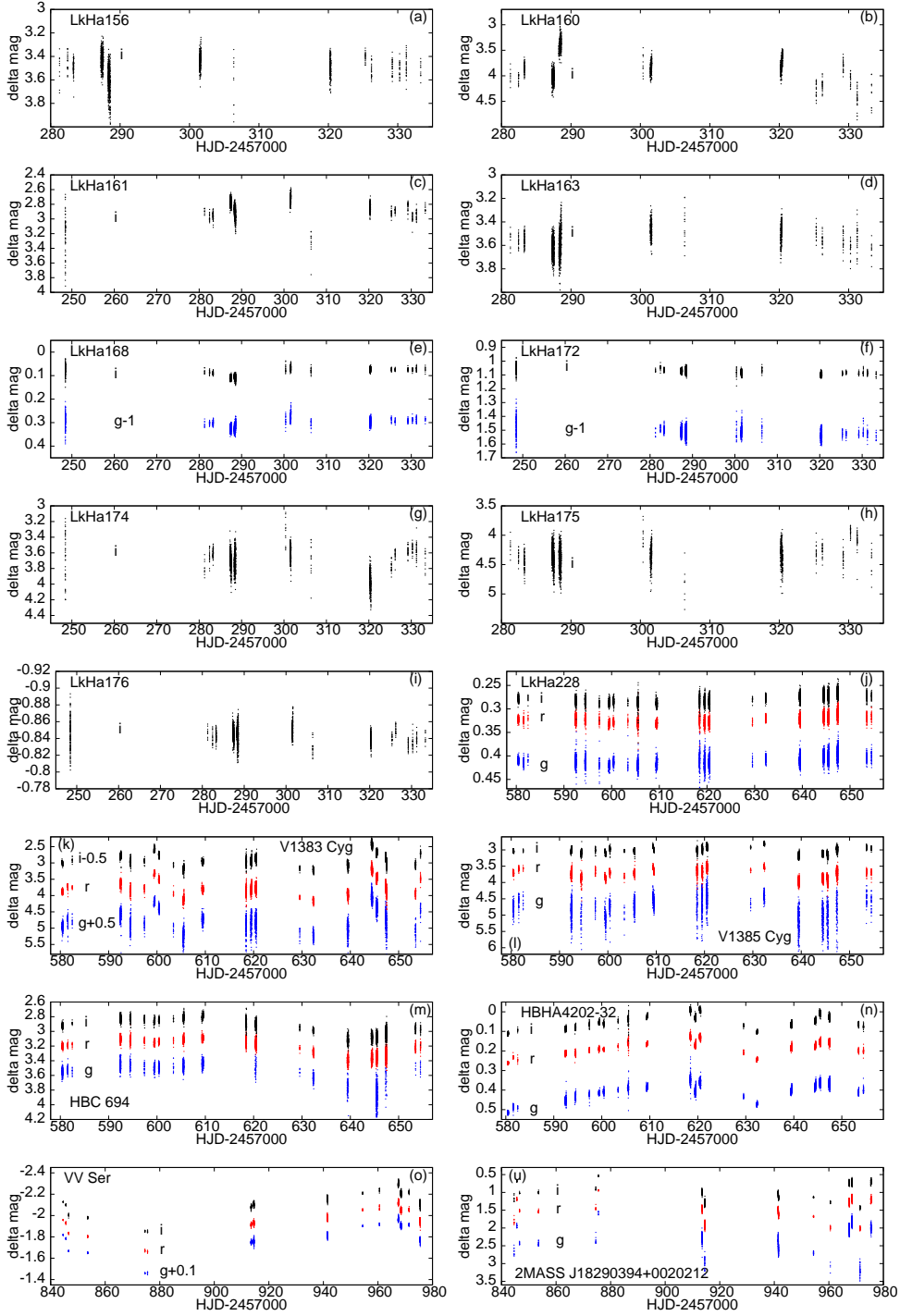


Fig. 13. Results for young variable stars from fields #7 and #9 in Cygnus and for the field #12.

- Bouvier, J., Matt, S. P., Mohanty, S., Scholz, A., Stassun, K. G., Zanni, C. Protostars and Planets VI, Henrik Beuther, Ralf S. Klessen, Cornelis P. Dullemond, and Thomas Henning (eds.), University of Arizona Press, Tucson, 914, **433**.
- Borucki, W. J., Koch D., Basri G., Batalha, M., Brown, T., et al. 2010, *Science*, **327**, 977.
- Boss, A. P. 2001, *ApJ*, **563**, 367.
- Chugainov, P. F., Zaitseva, G. V., Lovkaya, M. N. 1995, *AstL*, **21**, 457.
- Cody, A. M., Tayar, J., Hillenbrand, L. A., Matthews, J. M., Kallinger, T. 2013, *AJ*, **145**, 79.
- Crockett, C. J., Mahmud, N. I., Prato, L., Johns-Krull, C. M., et al. 2012, *ApJ*, **761**, 164.
- David, T. J., Hillenbrand, L. A., Petigura, E. A., et al. 2016, *Nature*, **534**, 658.
- Dahm, S. E., Hillenbrand, L. A. 2015, *AJ*, **149**, 200.
- Donati, J.-F., Hillébrard, E., Hussain, G. A. J., Moutou, C., et al. 2015, *MNRAS*, **453**, 3706.
- Donati, J.-F., Moutou, C., Malo, L., Baruteau, C., Yu, L., et al. 2016, *Nature*, **534**, 662.
- Drazkowska, J., Dullemond, C. P. 2018, *A&A*, **614**, 62.
- Frasca, A., Guillout, P., Klutsch, A., Freire Ferrero, R., et al. 2018, *A&A*, **612**, A96.
- Findeisen, K., Hillenbrand, L., Ofek, E., Levitan, D., et al. 2013, *ApJ*, **768**, 93.
- Flaherty, K. M., Muzerolle, J., Rieke, G., Gutermuth, R., et al. 2011, *ApJ*, **732**, 83.
- Ghosh, P., Lamb, F.K., Pethick, C.J. 1977, *ApJ*, **217**, 578.
- Gullbring, E., Barwig, H., Chen, P. S., Gahm, G. F., Bao, M. X. 1996, *A&A*, **307**, 791.
- Grankin, K. N., Melnikov, S. Yu., Bouvier, J., Herbst, W., Shevchenko, V. S. 2007, *A&A*, **461**, 183.
- Grankin, K. N., Bouvier, J., Herbst, W., Melnikov, S. Yu. 2008, *A&A*, **479**, 827.
- Grankin, K. N.; Shenavrin, V. I.; Irsamambetova, T. R.; Petrov, P. P. 2018, *IBVS*, **6253**, 1.
- Grinin, V. P., Kolotilov, E. A., Rostopchina, A. 1995, *A&AS*, **112**, 457.
- Herbst, W., Herbst, D. K., Grossman, E. J., Weinstein, D. 1994, *AJ*, **108**, 1906.
- Herbst, W., Shevchenko, V. S. 1999, *AJ*, **118**, 1043.
- Herbst, W., Bailer-Jones, C., Mundt, R., et al. 2002, *A&A*, **396**, 513.
- Ibryamov, S. I., Semkov, E. H., Peneva, S. 2014, *RAA*, **14**, 1264.
- Ibryamov, S. I., Semkov, E. H., Peneva, S. P. 2015, *BlgAJ*, **22**, 3.
- Ibryamov, S. I., Semkov, E. H. 2016, *BlgAJ*, **24**, 62.
- Ibryamov, S. I., Semkov, E. H., Milanov, T., Peneva, S. 2018, *BlgAJ*, **18**, 137.
- Johansen, A., Lambrechts, M. 2017, *Annual Review of Earth and Planetary Sciences*, **45**, 359.
- Johns-Krull, C. M., McLane, J. N., Prato, L., Crockett, C. J., et al. 2016a, *ApJ*, **826**, 206.
- Johns-Krull, C. M., Prato, L., McLane, J. N., Ciardi, D. R., et al. 2016b, *ApJ*, **830**, 15.
- Jurdana-Sepic, R., Munari, U., Antonucci, S., Giannini, T., Lorenzetti, D. 2018, *A&A*, **614**, 9.
- Karim, Md. T., Stassun, K. G., Briceno, C., Vivas, A. K., Raetz, S., et al. 2016, *AJ*, **152**, 198.
- Königl, A. 1991, *ApJ*, **370**, L39.
- Kulkarni, A. K., Romanova, M. M. 2008, *MNRAS*, **386**, 673.
- Kulkarni, A. K., Romanova, M. M. 2009, *MNRAS*, **398**, 701.
- Kun, M., Balog, Z., Kenyon, S. J., Mamajek, E. E., Gutermuth, R. A. 2009, *ApJS*, **185**, 451.
- Kurosawa, R., Romanova, M. M. 2013, *MNRAS*, **431**, 2673.
- Lagrange, A.-M., Meunier, N., Chauvin, G., Sterzik, M., et al. 2013, *A&A*, **559**, A83.
- Manoj, P., Bhatt, H. C., Maheswar, G., Muneer, S. 2006, *ApJ*, **653**, 657.
- Matsakos, T., Chieze, J.-P., Stehle, C., Gonzalez, M., et al. 2013, *A&A*, **557**, A69.
- McGinnis, P. T., Alencar, S. H. P., Guimaraes, M. M., Sousa, A. P., et al. 2015, *A&A*, **577**, A11.
- Mendigutia, I., Mora, A., Montesinos, B., Eiroa, C., et al. 2012, *A&A*, **543**, A59.
- Miroshnichenko, A.S., Yudin, R.V., Yakubov, S.D. 1992, *A&ATr*, **1**, 211.
- Motl, D. 2011, <http://c-munipack.sourceforge.net>.
- Muzerolle, J., Flaherty, K., Zoltan, B., Tracy, B., Gutermuth, R. 2019, *arxiv1904.06424*.
- Nelson, R. P., Papaloizou, J. C. B. 2003, *MNRAS*, **339**, 993.
- Neuhauser, R., Errmann, R., Berndt, A., Maciejewski, G., et al. 2011, *AN*, **332**, 547.
- Pavlova, L. A., Kondratyeva L. N., Valiullin R. R. 2005, *A&ATr*, **24**, 307.
- Perez, L. M., Carpenter, J. M., Andrews, S. M., Ricci, L., Isella, A., et al. 2016, *Sci*, **353**, 1519.
- Pigulski, A., Baran, A., Bzowski, M., Cugier, H., Czerny, B., et al. 2017, *Proceedings of the Polish*

Astronomical Society, **5**, 76.

- Poljancic Beljan, I., Jurdana-Sepic, R., Semkov, E. H., et al. 2014, *A&A*, **568**, A49.
- Pollack, J. B., Hubickyj, O., Bodenheimer, P., et al. 1996, *Icarus*, **124**, 62.
- Ricker, G. R., Winn, J. N., Vanderspek, R., et al. 2015, *JATIS*, **1**, 4003.
- Romanova, M. M., Ustyugova, G. V., Koldoba, A. V., Lovelace, R. V. E. 2004, *ApJ*, **610**, 920.
- Romanova, M. M., Lovelace, R. V. E. 2006, *ApJ*, **645**, L73.
- Romanova, M. M., Kulkarni, A. K., Lovelace, R. V. E. 2008, *ApJ*, **673**, L171.
- Romanova, M. M., Ustyugova, G. V., Koldoba, A. V., Lovelace, R. V. E. 2013, *MNRAS*, **430**, 699.
- Rucinski, S. M., Matthews, J. M., Kuschnig, R., Pojmanski, G., et al. 2008, *MNRAS*, **391**, 1913.
- Rucinski, S. M., Zwintz, K., Hareter, M., Pojmanski, G., et al. 2010, *A&A*, **522**, A113.
- de Sá, L., Chi  ze, J.-P., Stehl  , C., Hubeny, I., Lanz, T., Cayatte, V. 2019, *A&A*, **630**, A84.
- Semkov, E., Peneva S., Munari U., Milani A., Valisa P. 2010, *A&A*, **523**, 3.
- Semkov, E., Ibyamov, S. I., Peneva, S. P. 2017, *BlaAJ*, **27**, 75.
- Siwak, M., Rucinski, S. M., Matthews, J. M., Pojmanski, G., et al. 2011a, *MNRAS*, **410**, 2725.
- Siwak, M., Rucinski, S. M., Matthews, J. M., Kuschnig, R., et al. 2011b, *MNRAS*, **415**, 1119.
- Siwak, M., Rucinski, S. M., Matthews, J. M., Kuschnig, R., et al. 2014, *MNRAS*, **444**, 327.
- Siwak, M., Ogloza, W., Rucinski, S. M., Moffat, A. F. J., et al. 2016, *MNRAS*, **456**, 3972.
- Siwak, M., Ogloza, W., Moffat, A. F. J., Matthews, J. M., et al. 2018, *MNRAS*, **478**, 758.
- Stauffer, J., Cody, A. M., Baglin, A., Alencar, S., et al. 2014, *AJ*, **147**, 83.
- Stauffer, J., Cody, A. M., McGinnis, P., Rebull, L., et al., 2015, *AJ*, **149**, 130.
- Stetson, P. B. 1987, *PASP*, **99**, 191.
- Stolker, T., Dominik, C., Avenhaus, H., Min, M., de Boer, J., et al. 2016, *A&A*, **595**, 113.
- Strassmeier, K. G., Rice, J. B., Ritter, A., K  ker, M., et al. 2005, *A&A*, **440**, 1105.
- Tofflemire, B. M., Mathieu, R. D., Ardila, D. A., et al. 2017a, *ApJ*, **835**, 8.
- Tofflemire, B. M., Mathieu, R. D., Herczeg, G. J., Akeson, R. L., Ciardi, D. R. 2017b, *ApJ*, **842**, 12.
- van Eyken, J. C., Ciardi, D. R., von Braun, K., et al. 2012, *ApJ*, **755**, 42.
- Walker, M. F. 1980, *PASP*, **92**, 66.
- Warmels, R. H. 1991, *PASP Conf. Series*, **25**, 115.
- Yu, L., Winn, J. N., Gillon, M., Albrecht, S., Rappaport, S., et al. 2015, *ApJ*, **812**, 48.
- Yu, L., Donati, J.-F., Hebrard, E. M., Moutou, C., Malo, L., et al. 2017, *MNRAS*, **467**, 1342.

Table 1

Stars (column 2) observed in consecutive fields (column 1) and their coordinates in ICRS 2000 system (column 3 and 4). Classification given either in SIMBAD database, by other authors and/or firmly deduced from our light curves is given in column 5. In column 6 we indicate mechanism causing observed variability if firmly established, otherwise the question mark is present. Stars showing constant light during our monitoring (both in short and long time scales) are also indicated. Periods (in days) with errors in parentheses are given for eight periodic stars. Two FU Ori-type stars are marked in bold – data obtained during this survey will be the subject of separate study.

Field	Stars	RA [hh:mm:ss]	DEC [° :′ :″]	Classification	Variability
#1	VY Mon	06:31:06.92	+10:26:04.98	HAEBE	dipper
	V481 Mon	06:31:09.14	+10:26:10.73	CTTS	dipper
	V540 Mon	06:31:07.66	+10:26:19.85	CTTS	uncertain
	V541 Mon	06:31:07.96	+10:28:36.92	CTTS	dipper
	V542 Mon	06:31:15.74	+10:28:13.30	CTTS?	uncertain
	V687 Mon	06:31:10.13	+10:26:04.47	CTTS	dipper
	V698 Mon	06:30:50.17	+10:33:09.81	HAEBE	dipper
	LkHa 342	06:31:30.12	+10:32:33.55	CTTS	dipper
	2MASS J06310484+1027317	06:31:04.84	+10:27:31.81	YSO	uncertain
	2MASS J06311294+1027468	06:31:12.94	+10:27:46.92	YSO	dipper
	2MASS J06311457+1027305	06:31:14.57	+10:27:30.59	YSO	uncertain
	2MASS J06312223+1020134	06:31:22.24	+10:20:13.55	YSO	const.
	2MASS J06312967+1023230	06:31:29.67	+10:23:23.07	YSO	const.
	KHA 17	06:31:13.56	+10:26:59.99	YSO	uncertain
	KHA 22	06:31:37.49	+10:26:58.05	YSO?	uncertain
#2	V521 Cyg	20:58:23.81	+43:53:11.39	CTTS	dipper
	V1538 Cyg	20:57:57.51	+43:50:08.91	WTTS?	const., flare
	V1539 Cyg	20:57:59.88	+43:53:26.00	CTTS	accretor
	V1716 Cyg	20:58:06.12	+43:53:01.12	WTTS	4.16(9) d
	V1929 Cyg	20:57:22.25	+43:57:53.43	WTTS?	0.4263(15) d
	V1957 Cyg	20:57:56.52	+43:52:36.21	WTTS?	5.2875(80) d
	V2051 Cyg	20:57:48.81	+43:50:23.55	WTTS?	const., flare
	V2493 Cyg	20:58:17.03	+43:53:43.34	FUor	–
	LkHa 187	20:58:21.54	+43:53:44.89	CTTS?	dipper
	LkHa 189	20:58:24.01	+43:53:54.56	CTTS?	2.42(5) d
	LkHa 191	20:59:05.83	+43:57:03.14	CTTS	dipper
	2MASS J20573452+4359547	20:57:34.54	+43:59:54.72	YSO	uncertain
	[RGS2011]J205745.44+434845.1	20:57:45.44	+43:48:45.14	WTTS?	0.3692(15) d
	2MASS J20580604+4349328	20:58:06.06	+43:49:32.90	WTTS?	1.333(10) d
	2MASS J20580885+4346598	20:58:08.86	+43:46:59.84	CTTS?	5.85(1) d
	2MASS J20581082+4353082	20:58:10.82	+43:53:08.25	CTTS?	uncertain
	TYC 3179-925-1	20:57:17.48	+43:49:48.43	YSO	uncertain
#3	BM And	23:37:38.48	+48:24:11.84	CTTS	dipper
#4	GH Tau	04:33:06.22	+24:09:33.63	CTTS	dip/acc
	GI Tau	04:33:34.06	+24:21:17.07	CTTS	dip/acc
	GK Tau	04:33:34.56	+24:21:05.85	CTTS	dip/acc
	V807 Tau	04:33:06.63	+24:09:55.04	CTTS	accretor

Table 2

Table 1 - continuation

Field	Stars	RA [hh:mm:ss]	DEC [$^{\circ}$:':"]	Classification	Variability
#5	EH Cep	21:03:24.39	+67:59:06.52	CTTS	dipper
	FU Cep	21:01:46.75	+68:08:45.24	CTTS	accretor
	FW Cep	21:02:33.01	+68:07:29.10	CTTS	dipper
	HZ Cep	21:01:36.2	+68:08:22.00	CTTS	accretor
	SX Cep	21:01:37.57	+68:11:30.95	WTTS?	uncertain
	LkHa 428 N+S	21:02:28.30	+68:03:28.52	CTTS?	uncertain
	2MASS J21005550+6811273	21:00:55.56	+68:11:27.21	CTTS?	uncertain
	2MASS J21005808+6809382	21:00:58.13	+68:09:38.21	CTTS?	uncertain
	2MASS J21010367+6813092	21:01:03.72	+68:13:09.26	CTTS?	dipper?
	2MASS J21011252+6810195	21:01:12.53	+68:10:19.52	CTTS?	uncertain
	2MASS J21012706+6810381	21:01:27.06	+68:10:38.11	CTTS?	uncertain
	2MASS J21014250+6812572	21:01:42.51	+68:12:57.25	CTTS?	uncertain
	2MASS J21014358+6809361	21:01:43.59	+68:09:36.18	WTTS?	uncertain
	2MASS J21025943+6806322	21:02:59.44	+68:06:32.24	CTTS?	uncertain
	unnamed	21:01:05.19	+68:04:21.79	CTTS?	dipper
#6	DI Cep	22:56:11.54	+58:40:01.77	CTTS	accretor
#7	LkHa 156	20:51:26.99	+44:13:15.45	CTTS?	uncertain
	LkHa 160	20:51:41.42	+44:15:07.10	CTTS?	accretor?
	LkHa 161	20:51:41.91	+44:16:08.20	CTTS?	uncertain
	LkHa 163	20:51:58.65	+44:14:56.75	CTTS?	uncertain
	LkHa 168	20:52:06.05	+44:17:16.04	HAEBE	uncertain
	LkHa 172	20:52:26.76	+44:17:06.63	CTTS	const.?
	LkHa 174	20:52:30.89	+44:20:11.62	CTTS?	uncertain
	LkHa 175	20:52:34.37	+44:17:40.26	CTTS?	uncertain
	LkHa 176	20:52:58.83	+44:15:03.79	HAEBE	uncertain
	2MASS J20523726+4418145	20:52:37.27	+44:18:14.52	YSO?	const.?
#8	DD Tau	04:18:31.13	+28:16:29.16	CTTS	accretor
	CY Tau	04:17:33.73	+28:20:46.81	CTTS	accretor
	CZ Tau	04:18:31.59	+28:16:58.16	CTTS	uncertain
	V892 Tau	04:18:40.61	+28:19:15.64	CTTS	const.
	V1023 Tau	04:18:47.03	+28:20:07.49	CTTS	accretor
#9	LkHa 228	20:24:31.02	+42:16:05.07	CTTS	uncertain
	HBC 694	20:24:29.54	+42:14:02.00	HAEBE	dipper?
	V1515 Cyg	20:23:48.02	+42:12:25.78	FUor	–
	HBHA 4202-32	20:24:23.05	+42:20:02.82	HAEBE	dipper?
	[D75b] Em*20-080	20:24:22.35	+42:16:53.80	HAEBE	const.
	V1383 Cyg	20:24:11.20	+42:17:09.10	CTTS?	accretor
	V1385 Cyg	20:24:39.59	+42:21:09.02	CTTS?	uncertain

Table 3

Table 1 - continuation

Field	Stars	RA [hh:mm:ss]	DEC [° :':"]	Classification	Variability
#10	HI Ori	05:31:23.59	+12:09:43.83	CTTS	dipper
	HK Ori	05:31:28.05	+12:09:10.15	CTTS?	dipper
	HM Ori	05:31:47.80	+12:18:08.20	CTTS?	dipper
	V448 Ori	05:30:51.70	+12:08:36.73	CTTS	accretor
	V450 Ori	05:31:24.55	+12:12:11.01	CTTS	dipper
	2MASS J05315128+1216208	05:31:51.29	+12:16:20.75	CTTS	dipper
	[DM99] 135	05:31:08.02	+12:06:06.37	CTTS?	const.
	[DM99] 136	05:31:15.50	+12:11:23.70	CTTS	dipper
	[DM99] 142	05:31:21.66	+12:05:47.69	CTTS?	uncertain
	[DM99] 152	05:31:40.48	+12:10:46.88	WTTS?	uncertain
	[DM99] 161	05:31:58.48	+12:22:47.36	WTTS?	const.
	[DM99] 164	05:31:59.94	+12:08:06.80	WTTS?	uncertain
#11	V350 Cep	21:42:59.99	+66:11:27.90	CTTS	uncertain
	V361 Cep	21:42:50.18	+66:06:35.18	HAEBE	uncertain
	V373 Cep	21:43:06.82	+66:06:54.24	HAEBE	uncertain
	BD+65 1636	21:42:46.04	+66:05:13.80	HAEBE	const.
	BD+65 1638	21:42:58.56	+66:06:10.56	HAEBE	uncertain
	2MASS J21424031+6610069	21:42:40.31	+66:10:07.00	YSO	const.
	2MASS J21424705+6604578	21:42:47.06	+66:04:57.90	YSO	dipper?
	2MASS J21424707+6610512	21:42:47.07	+66:10:51.30	YSO?	const.
	2MASS J21425349+6608053	21:42:53.48	+66:08:05.29	YSO?	uncertain
	2MASS J21430168+6607089	21:43:01.68	+66:07:08.96	YSO	const.
	2MASS J21431161+6609114	21:43:11.59	+66:09:11.46	YSO?	uncertain
	2MASS J21432695+6609365	21:43:26.95	+66:09:36.45	YSO	const.
	2MASS J21432932+6603319	21:43:29.34	+66:03:31.96	YSO	const.
	2MASS J21433625+6611329	21:43:36.25	+66:11:32.89	YSO	uncertain
#12	2MASS J21435035+6608477	21:43:50.36	+66:08:47.65	YSO?	uncertain
	TYC 4261-842-1	21:42:26.93	+66:07:42.60	YSO?	const.
	VV Ser	18:28:47.86	+00:08:39.92	HAEBE	dipper
	2MASS J18282143+0010409	18:28:21.45	+00:10:41.14	CTTS?	const.
	2MASS J18285808+0017243	18:28:58.09	+00:17:24.38	CTTS?	const.
	2MASS J18290025+0016578	18:29:00.25	+00:16:57.85	CTTS?	const.
#13	2MASS J18290394+0020212	18:29:03.94	+00:20:21.26	CTTS?	accretor
	2MASS J18290576+0022324	18:29:05.77	+00:22:32.41	YSO	const.
	LkHa 208	06:07:49.53	+18:39:26.49	HAEBE	uncertain
#14	LkHa 209	06:08:14.39	+18:37:25.00	CTTS?	uncertain
	DI Tau	04:29:42.47	+26:32:49.12	CTTS	const.
#15	DH Tau	04:29:41.56	+26:32:58.27	CTTS	accretor
	JH 507	04:29:20.70	+26:33:40.44	CTTS	accretor
	2MASS J04293623+2634238	04:29:36.24	+26:34:23.49	CTTS	const.
	V395 Cep	23:20:52.12	+74:14:07.08	CTTS	3.42(1) d

Table 4

Table 1 - continuation. Stars observed with 20-cm telescope.

Field	Stars	RA [hh:mm:ss]	DEC [$^{\circ}$: $'$: $''$]	Classification	Variability
#16	BH Cep	22:01:42.87	+69:44:36.42	HAEBE	uncertain
#17	HD 174571	18:50:47.17	+08:42:10.09	HAEBE	uncertain
#18	HD 190073	20:03:02.51	+05:44:16.66	HAEBE	uncertain
#19	HD 203024	21:16:03.05	+68:54:52.10	HAEBE	uncertain
#20	V594 Cas	00:43:18.26	+61:54:40.14	HAEBE	uncertain

Table 5

Log of observations. Field names, dates of observations and filters used during given observation are listed in consecutive columns.

Field No.	Comp. stars	Date [yyyy.mm.dd]	Filters	Date [yyyy.mm.dd]	Filters
# 1 0.9 d	3UC 202-059221	2013.02.11	BVRI	2014.02.06	VI
	3UC 201-058983	03.28	BVRI	02.07	VI
		03.02	BVRI	02.08	VI
		03.04	BVRI	02.10	VI
		03.05	BVRI	2015.03.07	I
		03.06	BVRI	03.08	I
		03.16	BVRI	03.09	I
		03.17	BVRI	03.10	I
		12.27	BVI	03.16	I
		2014.01.07	BVI	03.17	I
		02.03	VI	03.20	I
		02.05	VI		
#2 0.96 d	3UC 268-201607	2013.07.18	BVRI	2013.08.25	BVRI
	3UC 268-201639 3UC 268-201660	07.19	BVRI	08.27	BVRI
		07.20	BVRI	09.03	BVRI
		07.21	BVRI	09.04	BVRI
		07.22	BVRI	09.05	BVRI
		07.23	BVRI	09.06	BVRI
		07.24	BVRI	09.07	BVRI
		07.25	BVRI	09.08	BVRI
		07.26	BVRI	09.10	BVRI
		07.27	BVRI	09.13	BVRI
		07.28	BVRI	09.14	VRI
		08.01	BVRI	09.30	VRI
		08.02	BVRI	10.10	VRI
		08.03	BVRI	10.11	VRI
		08.04	BVRI	10.12	VRI
		08.05	BVRI	10.13	VRI
		08.06	BVRI	10.14	VRI
		08.07	BVRI	10.15	VRI
		08.08	BVRI	10.17	VRI
		08.15	BVRI	10.19	BVRI
		08.16	BVRI	10.20	BVRI
		08.17	BVRI	10.21	BVRI
		08.18	BVRI	10.25	BVRI
		08.22	BVRI	10.26	BVRI
		08.23	BVRI	10.27	BVRI
		08.24	BVRI	10.28	BVRI
#3 0.48 d	TYC 3642-1917-1	2013.09.10	VRI	2013.10.22	BVI
	3UC 277-285405	09.30	BVRI	10.23	BVI
		10.10	BVI	10.24	BVI
		10.12	BVI	11.08	BVI
		10.13	BVI	11.12	BVI
		10.15	BVI	11.14	BVI
		10.20	BVI	11.16	BVI
		10.21	BVRI	11.17	BVI

Table 6
Table 5b - continuation.

Field	Comp. stars	Date [yyyy.mm.dd]	Filters	Date [yyyy.mm.dd]	Filters
#4 0.83 d	3UC 229-025810	2013.11.07	BVI	2013.12.24	BVI
	TYC 1829-186-1	11.08	BVI	12.27	BVI
		12.03	BVI	12.28	BVI
		12.12	BVI	12.31	BVI
		12.13	BVI	2014.01.02	BVI
		12.18	BVI	01.03	BVI
		12.19	BVI	01.06	BVI
		12.23	BVI	01.07	BVI
#5 0.93 d	3UC 317-077414	2014.08.02	gri	2014.11.02	gi
	3UC 317-077395	09.19	gri	11.23	gi
	3UC 317-077386	09.20	gri	2016.09.26	gri
		10.27	gi	09.27	gri
		10.28	gi	09.29	gri
		10.29	gi	09.30	gri
		10.30	gi	10.01	gri
		10.31	gi		
#6 0.75 d	GSC 3997-1833	2014.11.03	gri	10.30	gri
	GSC 3997-2030	11.09	gri	11.02	gri
	3UC 298-177839	12.04	gri	11.03	gri
	3UC 298-177787	12.05	gri	11.08	gri
		2015.10.27	gri	11.24	gri
		10.29	gri	11.25	gri
#7 0.49 d	TYC 3179-198-1	2015.08.13	gi	2015.10.10	gi
	USNO-A2 1275-14250279	09.15	gi	10.24	gi
		09.16	gi	10.29	gi
		09.17	gi	10.30	gi
		09.21	gi	11.02	gi
		09.22	gi	11.03	gi
		10.04	gi	11.04	gi
		10.05	gi	11.06	gi
#8 0.90 d	2MASS J0418423+281140	2015.12.19	gri	2016.12.20	gri
	JH 161	12.20	gri	12.21	gri
		12.29	gri	12.30	gri
		12.30	gri	12.31	gri
		2016.12.05	gri	2017.01.01	gri
		12.07	gri		
#9 1.24 d	TYC 3160-1814-1	2016.07.10	gri	2016.08.17	gri
	3UC 265-198648	07.11	gri	08.18	gri
		07.12	gri	08.19	gri
		07.22	gri	08.28	gri
		07.24	gri	08.31	gri
		07.27	gri	09.07	gri
		07.29	gri	09.12	gri
		07.30	gri	09.13	gri
		08.02	gri	09.15	gri
		08.04	gri	09.21	gri
		08.08	gri	09.22	gri

Table 7
Table 5c - continuation.

Field	Comp. stars	Date [yyyy.mm.dd]	Filters	Date [yyyy.mm.dd]	Filters
#10 0.80 d	USNO-A2 0975-01667849	2016.12.29	gri	2017.02.13	gri
		2017.01.19	gri	02.15	gri
	USNO-A2 0975-01682657	01.22	gri	02.25	gri
		01.28	gri	2018.01.14	gri
		02.11	gri	01.15	gri
		02.12	gri	01.16	gri
#11 0.70 d	TYC 4274-1993-1	2015.09.16	gi	2015.11.06	gi
		09.17	gi	11.08	gi
	USNO-A2 1500-08311095	09.21	gi	2017.08.30	gri
		10.10	gi	08.31	gri
		10.24	gi	09.30	gri
		10.29	gi	10.01	gri
		10.30	gi	10.18	gri
		11.02	gi	11.04	gri
		11.03	gi	11.05	gri
		11.04	gi	12.13	gri
#12 0.45 d	USNO-A2 0900-12955282	2017.03.31	gri	2017.06.09	gri
		04.01	gri	07.06	gri
	USNO-A2 0900-12947374 USNO-A2 0900-12917818	04.02	gri	07.19	gri
		04.09	gri	07.25	gri
		04.30	gri	08.01	gri
		05.01	gri	08.02	gri
		05.27	gri	08.05	gri
		06.08	gri	08.09	gri
#13 0.42 d	TYC 1318-514-1	2017.01.19	gri	2017.03.24	gri
		01.20	gri	03.27	gri
		01.22	gri	03.28	gri
		01.28	gri	03.31	gri
		02.12	gri	04.01	gri
		02.13	gri	2018.02.19	gri
		02.25	gri		
#14 0.48 d	XEST 15-OM-160 XEST 15-OM-056	2018.02.16	gri	2018.11.29	BVI
		03.01	gri	11.30	BVI
		03.03	gri		
#15 0.72 d	TYC 4490-1027-1 TYC 4490-1174-1 TYC 4490-1241-1	2018.11.05	vby	2018.11.10	vby
		11.07	vby	11.11	vby
		11.08	vby	11.12	vby
#16	TYC 4467-312-1 TYC 4466-384-1	2017.07.18	BV	2017.07.21	BV
		07.19	BV	07.23	BV
		07.20	BV		
#17	HD 174587 TYC 1026-2089-1	2017.07.29	BV	2018.08.05	BV
		07.30	BV	08.07	BV
		07.31	BV	08.08	BV
		08.01	BV	08.09	BV
#18	HD 189851 HD 189823	2017.09.04	BV	2017.09.29	BV
		09.07	BV	09.30	BV
		09.27	BV	10.01	BV
		09.28	BV		
#19	BD+68 1118 TYC 4461-1154-1	2017.08.14	BV	2017.08.26	BV
		08.20	BV	08.28	BV
		08.23	BV	09.04	BV
		08.24	BV		
#20	BD+61 155 TYC 4020-1206-1	2017.10.15	BV	2017.10.17	BV
		10.16	BV		